

Discovery and Preclinical Pharmacology of a Selective ATP-Competitive Akt Inhibitor (GDC-0068) for the Treatment of Human Tumors

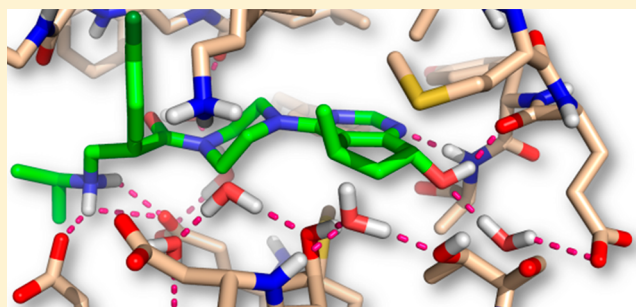
James F. Blake,^{*,†} Rui Xu,[†] Josef R. Bencsik,[†] Dengming Xiao,[†] Nicholas C. Kallan,[†] Stephen Schlachter,[†] Ian S. Mitchell,[†] Keith L. Spencer,[†] Anna L. Banka,[†] Eli M. Wallace,[†] Susan L. Gloor,[†] Matthew Martinson,[†] Richard D. Woessner,[†] Guy P.A. Vigers,[†] Barbara J. Brandhuber,[†] Jun Liang,[‡] Brian S. Safina,[‡] Jun Li,[‡] Birong Zhang,[‡] Christine Chabot,[‡] Steven Do,[‡] Leslie Lee,[‡] Jason Oeh,[‡] Deepak Sampath,[‡] Brian B. Lee,[‡] Kui Lin,[‡] Bianca M. Liederer,[‡] and Nicholas J. Skelton[‡]

[†]Array BioPharma Inc., 3200 Walnut Street, Boulder, Colorado 80301, United States

[‡]Genentech Inc., 1 DNA Way, South San Francisco, California 94080-4990, United States

S Supporting Information

ABSTRACT: The discovery and optimization of a series of 6,7-dihydro-*S*H-cyclopenta[*d*]pyrimidine compounds that are ATP-competitive, selective inhibitors of protein kinase B/Akt is reported. The initial design and optimization was guided by the use of X-ray structures of inhibitors in complex with Akt1 and the closely related protein kinase A. The resulting compounds demonstrate potent inhibition of all three Akt isoforms in biochemical assays and poor inhibition of other members of the cAMP-dependent protein kinase/protein kinase G/protein kinase C extended family and block the phosphorylation of multiple downstream targets of Akt in human cancer cell lines. Biological studies with one such compound, **28** (GDC-0068), demonstrate good oral exposure resulting in dose-dependent pharmacodynamic effects on downstream biomarkers and a robust antitumor response in xenograft models in which the phosphatidylinositol 3-kinase–Akt–mammalian target of rapamycin pathway is activated. **28** is currently being evaluated in human clinical trials for the treatment of cancer.



INTRODUCTION

Protein kinase B (PKB)/Akt is a serine–threonine kinase, a downstream target for phosphatidylinositol 3-kinase (PI3K), which comprises three closely related isoforms (Akt1, Akt2, and Akt3). Akt functions as a pivotal node in the PI3K–Akt–mTOR pathway; once activated, Akt can control key cellular processes by phosphorylating substrates involved in apoptosis, transcription, cell cycle progression, and translation.¹ Akt activity is frequently elevated in cancer due to amplification and/or gain-of-function mutations of upstream receptor tyrosine kinases and/or PI3K, as well as loss of PTEN function, a negative regulator of Akt.² Constitutive activation or overexpression of Akt isoforms has been identified in a wide variety of human tumors, including breast, prostate, ovarian carcinoma, and melanoma.² shRNA knockdown of Akt in PTEN-null tumor xenograft models demonstrates antitumor effects with maximum efficacy achieved by inhibiting all three isoforms.³ Combined, these factors contribute to the attractiveness of inhibiting Akt activity as a novel therapeutic approach to cancer treatment.⁴

Strategies for targeting Akt have included both ATP-competitive, active-site-directed inhibitors, and non-ATP-

competitive allosteric compounds. Several advanced Akt inhibitors, representing both classes of compounds, were or are being tested in clinical trials for the treatment of human cancers.⁵ Herein, we report on the discovery and preclinical characterization of **28** (GDC-0068), a highly selective pan-Akt inhibitor that targets the ATP-binding cleft.

As detailed in previous work,^{6,7} compounds exemplified by **1** and **2** (Figure 1) demonstrated potent inhibition of Akt in biochemical assays (Akt1 enzyme inhibition, IC₅₀, of 3 and 1 nM for **1** and **2**, respectively), reduced phosphorylation of Akt substrates in cellular assays (e.g., reduction of p-PRAS40 levels in LNCaP cells with IC₅₀ values of 160 and 137 nM for **1** and **2**, respectively), and down-regulation of Akt signaling in xenograft models of human cancer in nude mice. While the lack of kinase selectivity and resulting tolerability issues hindered the development of **1**, compound **2** displayed a significantly improved selectivity profile versus kinases such as PKA (PKA enzyme inhibition IC₅₀/Akt1 enzyme inhibition IC₅₀ = 35), ROCK1, and

Received: July 12, 2012

Published: August 30, 2012

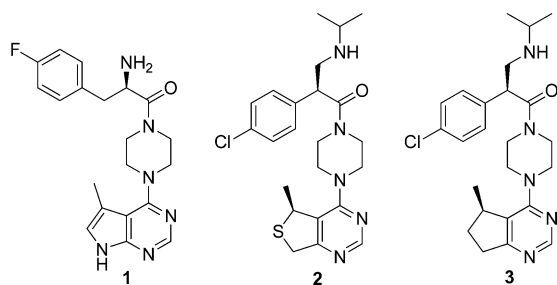


Figure 1. Advanced proof-of-concept pan-Akt inhibitors.

other related AGC family members and was well tolerated while showing significant antitumor activity in PC3-NCI prostate cancer xenograft models.⁷ The present work builds on our experiences with **1** and **2** and utilizes the dihydrocyclopentapyrimidine core (exemplified by **3**) as a platform to further explore the selective inhibition of Akt. With suitable substitution around this core, potent Akt-selective compounds have been identified that exhibit druglike properties and are suitable candidates for clinical evaluation.

CHEMISTRY

The general synthetic routes used to prepare 6,7-dihydro-5H-cyclopenta[*d*]pyrimidine derivatives are outlined in the following schemes.

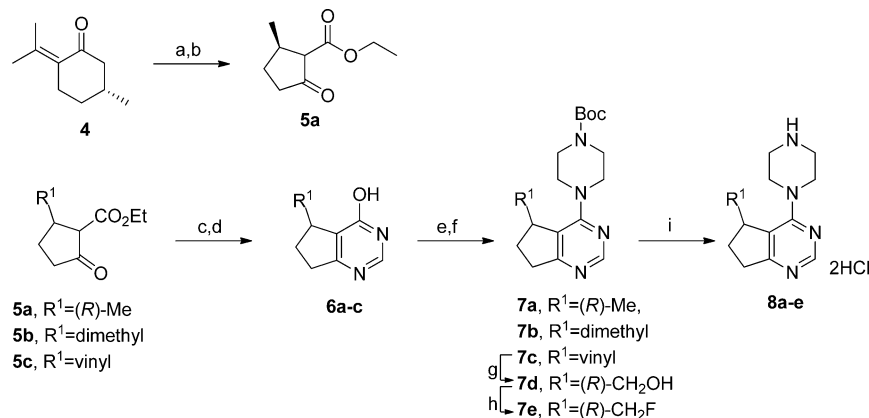
As shown in Scheme 1, preparation of the 5(*R*)-methyl-substituted cyclopenta[*d*]pyrimidine core requires rapid access to the β -keto ester intermediate **5a**. We decided to capitalize on the commercially available natural product chiral pool. Specifically, we searched for a starting material that could be readily manipulated into the desired β -keto ester, while allowing us to incorporate the desired methyl stereochemistry. Thus, commercially available (+)-pulegone (**4**) was sequentially reacted with bromine and sodium ethoxide to smoothly undergo ring contraction via a Favorskii rearrangement. Subsequent ozonolysis and reduction with zinc dust in acetic acid gave the desired chiral keto ester **5a** in excellent yield. Construction of the pyrimidine ring was carried out by initial conversion of β -keto esters **5a**, **5b**,⁸ and **5c**⁹ to enamines by ammonium acetate

followed by cyclization upon heating with formamide and ammonium formate to deliver pyrimidones **6a–c**. Phosphorous oxychloride-mediated chlorination followed by SnAr introduction of the Boc-protected piperazine linker delivered **7a–c**. Olefin **7c** was converted to alcohol **7d** by ozonolysis, followed by reductive workup with NaBH₄ and chiral supercritical fluid chromatography (SFC) separation of the resulting racemic alcohol. **7d** was then further functionalized by treatment with *n*-perfluorobutanesulfonyl fluoride (PBSF) and HF–Et₃N¹⁰ to afford **7e**. Removal of the Boc group in **7a–e** provided **8a–e** as dihydrochloride salts.

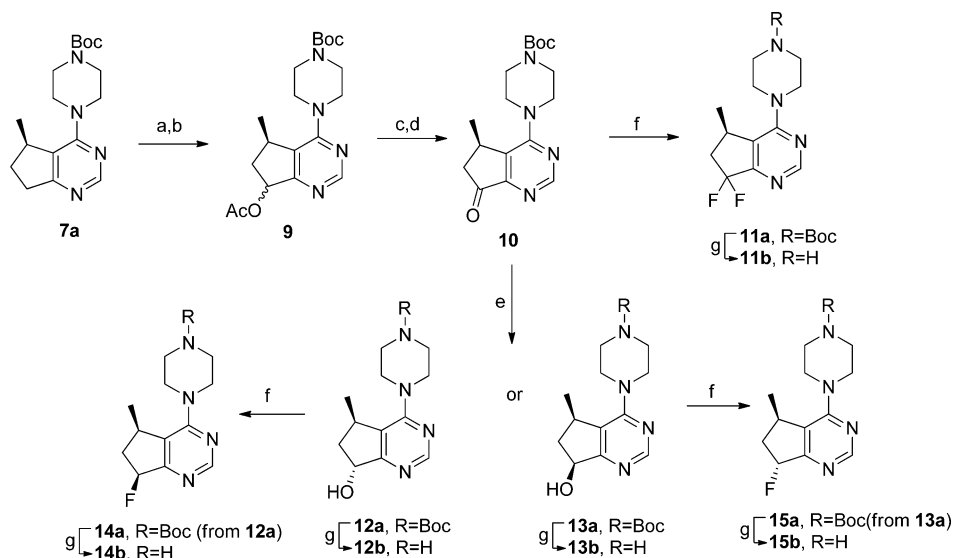
C7-hydroxylated and -fluorinated cyclopenta[*d*]pyrimidine cores were synthesized as illustrated in Scheme 2. Introduction of the C7-hydroxyl functionality was facilitated by *N*-oxide formation of **7a** followed by *N*-oxide acylation and concomitant rearrangement upon heating to give acetate **9** in a 3:2 *cis–trans* orientation. Hydrolysis of the acetate and subsequent Swern oxidation led to ketone **10**. Asymmetric transfer hydrogenation¹¹ using a ruthenium catalyst, RuCl(*p*-cymene)[(*R,R*)-TsDPEN], gave the desired (*R*)-alcohol **12a** in diastereomeric excess ranging from 94% to 98%. To obtain diastereomerically pure material, the alcohol was converted to the *p*-nitrophenyl ester, which enabled separation by either column chromatography or recrystallization. Hydrolysis of the *p*-nitrophenyl ester followed by acid-mediated *N*-Boc deprotection revealed the key amine intermediate **12b** in excellent diastereomeric excess (>99% by HPLC) as the dihydrochloride salt. The (*S*)-alcohol intermediate **13b** was prepared in a similar manner except for using the *S,S* ruthenium catalyst in the asymmetric hydrogenation step. Ketone **10**, (*R*)-alcohol **12a**, and (*S*)-alcohol **13a** were treated with DAST¹² to give the corresponding fluorinated products, which were deprotected under acidic conditions to yield the difluoro core **11b**, *cis*-fluoro core **14b**, and *trans*-fluoro core **15b**.

In Scheme 3, a convenient method for the preparation of optically active β -phenylalanine amino acids is described. The Evans auxiliary (*R*)-4-benzyloxazolidin-2-one (**16**) was coupled with 2-(4-chlorophenyl)acetyl chloride to give oxazolidin-2-one (**17**). Treatment of **17** with TiCl₄ at –78 °C followed by Mannich reaction of the resulting titanium enolate with *N*-acyliminium ions generated in situ from *N*-(alkoxymethyl)-

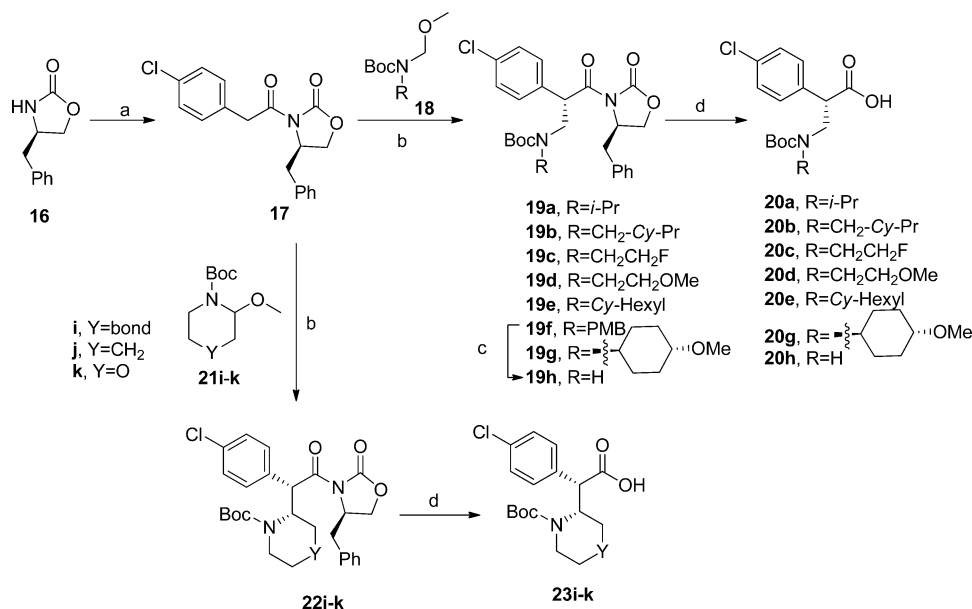
Scheme 1. Synthesis of 5-Substituted 6,7-Dihydro-5H-cyclopenta[*d*]pyrimidine Cores^a



^aReagents and conditions: (a) (i) NaHCO₃, Et₂O, Br₂, 0 °C; (ii) 21% NaOEt, EtOH, 0 °C to rt, 12 h; (iii) semicarbazide hydrochloride, NaOAc, H₂O–EtOH (2:1), reflux to rt, 12 h (64%); (b) (i) ozone, EtOAc, –78 °C; (ii) zinc dust, acetic acid, 0 °C, 2 h (94%); (c) NH₄OAc, MeOH, 12 h; (d) NH₄CO₂, formamide, 150 °C, 24 h; (e) POCl₃, DCE, reflux, 6 h; (f) *tert*-butyl piperazine-1-carboxylate, DIEA, 1-BuOH, reflux, 16 h; (g) (i) ozone, DCM, –78 °C, 15 min; (ii) EtSMe, rt, 1 h; (iii) NaBH₄, MeOH, 0 °C, 2 h (55%); (iv) chiral SFC separation; (h) PBSF, HF–Et₃N, (80%); (i) 4 N HCl in dioxane, DCM, 12 h.

Scheme 2. Synthesis of C7-Hydroxylated and -Fluorinated Cyclopenta[*d*]pyrimidine Cores^a

^aReagents and conditions: (a) *m*-CPBA, NaHCO₃, CHCl₃, 0 °C to rt, 2 h (100%); (b) acetic anhydride, 100 °C, 2 h (89%); (c) LiOH, THF–H₂O (5:1), 16 h (99%); (d) oxalyl chloride, DMSO, Et₃N, DCM, –78 °C to rt, 12 h (71%); (e) (i) RuCl(*p*-cymene)[(R,R)-TsDPEN] (for **12a**) or RuCl(*p*-cymene)[(S,S)-TsDPEN] (for **13a**), formic acid, Et₃N, DCM, 12 h (ii) 4-nitrobenzoyl chloride, Et₃N, DCM, 0 °C to rt, 4 h; (iii) LiOH, THF–H₂O (2:1), 0 °C to rt, 1 h; (f) DAST, DCM, –20 °C, 1 h; (g) 4 N HCl in dioxane, DCM, 12 h.

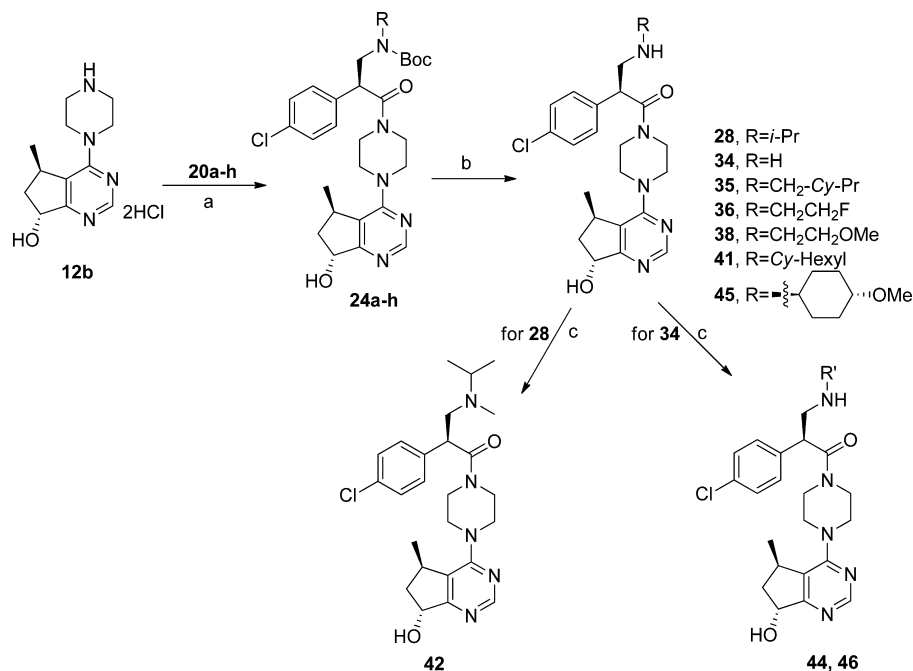
Scheme 3. Stereoselective Synthesis of β -Phenylalanine Amino Acids^a

^aReagents and conditions: (a) *n*-BuLi, THF, –78 to –20 °C, 2-(4-chlorophenyl)acetyl chloride, 12 h (79%); (b) 1 M TiCl₄, DCM, –78 °C, DIEA, rt, 1.5 h (72%); (c) DDQ, DCM, H₂O, 19 h (100%); (d) LiOH–H₂O, THF–H₂O (3:1), 0 °C, H₂O₂, 12 h.

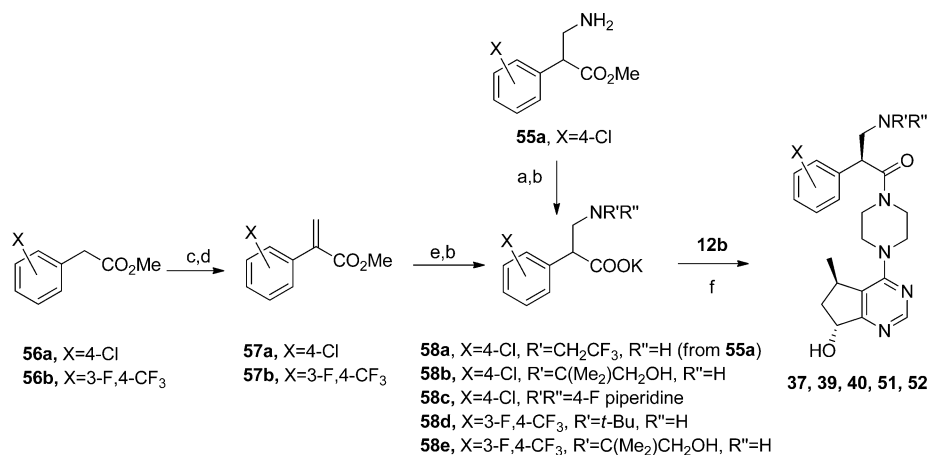
carbamates **18** afforded **19a–g** in good yield and diastereoisomeric ratio (for example, 14:1 diastereomeric excess (de) for **19a**). The diastereomers were easily separated by silica gel column chromatography. Basic hydrolysis of the chiral auxiliary provided the desired β -amino acids in excellent enantiopurity. *N*-Unsubstituted amino acid **20h** was synthesized by sequential cleavage of the *p*-methoxybenzyl ether (PMB) group and the chiral auxiliary in **19f**. In a similar manner, preparation of amino acids **23i–k** with cyclic amines was accomplished by stereoselective coupling of the Evans imide **17** with α -methoxy heterocycles **21i–k** followed by basic hydrolysis of the oxazolidinone auxiliary.¹³

With the requisite cores and β -phenylalanine amino acids in hand, preparation of the desired compounds was achieved by amide coupling, followed by Boc deprotection under acidic conditions, as exemplified in Scheme 4. The primary and secondary amines were further elaborated by reductive amination with Na(OAc)₃BH and aldehydes or ketones to afford the corresponding substituted amines.

Several analogues with CH₂CF₃- and *t*-Bu-substituted amines or cyclic tertiary amines were synthesized by an alternative route as outlined in Scheme 5. Alkylation of the primary amine **55a** with trifluoroethyl triflate followed by saponification of the methyl ester with KO(TMS) afforded **58a** as a potassium salt.

Scheme 4. Amide Coupling and Further Elaboration of Amines^a

^aReagents and conditions: (a) HBTU, Hünig's base, DCM, 1 h; (b) 4 N HCl, DCM, rt; (c) aldehyde or ketone, Na(OAc)₃BH, Hünig's base, DCE, rt, 16 h.

Scheme 5. Alternative Synthesis of Substituted Amines^a

^aReagents and conditions: (a) CF₃CH₂OTf, Hünig's base, THF-DMF (1:1), rt, 20 h, (93%); (b) KO(TMS), THF, rt, 18 h; (c) paraformaldehyde, 10% NaOMe, DMSO, rt, 12 h; (d) MsCl, TEA, DCM, 0 °C to rt, 12 h; (e) HNR'R'', THF, 0 °C, 12 h; (f) (i) HBTU, Hünig's base, DMF, 18 h; (ii) chiral separation.

Alternatively, phenyl acetate esters **56a,b** were converted to the acrylates **57a,b** as previously reported.^{6,7} Michael addition of amines followed by hydrolysis of the methyl ester provided **58b-e** as racemates, which were then coupled with the C7-hydroxylated core **12b**. Finally, all diastereomeric pairs were resolved by chiral stationary-phase HPLC or chiral SFC to obtain desired compounds **37**, **39**, **40**, **51**, and **52**. The stereochemical assignments of compounds **37**, **39**, **40**, **51**, and **52** were based on the results of the Akt1 enzyme inhibition assay. All diastereomeric pairs were tested, and the active diastereomer was then assigned the stereochemistry shown in Scheme 5 on the basis of the activity of highly similar compounds prepared enantioselectively.

RESULTS AND DISCUSSION

Analysis of a series of X-ray structures of the pyrrolopyrimidine and dihydrothienopyrimidine hinge-binding cores bound to Akt1 and PKA suggested that increased steric bulk near the gatekeeper residue tended to improve the selectivity profile relative to PKA and ROCK1/2. This was principally due to differences between Akt1 and PKA that include Thr211 (Akt1) to Val (PKA), Met281 (Akt1) to Leu, and Ala230 (Akt1) to Val, which lead to a narrower and less polar cavity in PKA, which should be less forgiving of larger hinge-binding functionality (cf. Figure 2, ref 7). The saturated ring and larger sulfur atom of dihydrothienopyrimidine **2** confer 35-fold selectivity for Akt1 versus PKA, while pyrrolopyrimidine **1** is only 2-fold selective. The increased polarity of the Akt1 active site conferred by

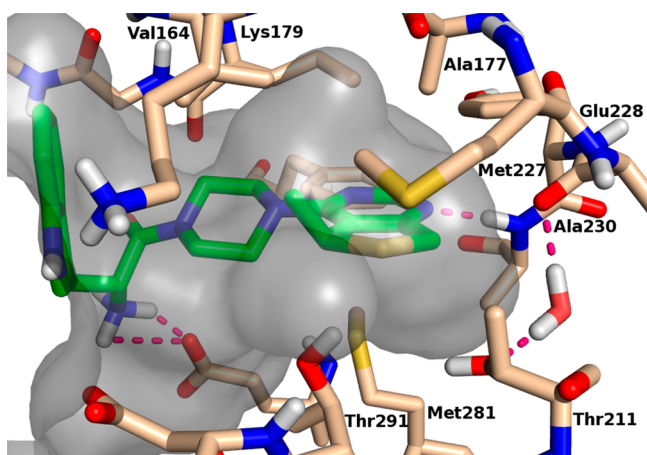


Figure 2. X-ray crystal structure of Akt1 in complex with a dihydrothienopyrimidine inhibitor (compound 26 from ref 7, PDB code 3OW4) at 2.6 Å resolution showing the molecular surface of the pocket in the vicinity of the hinge (hydrogens added for clarity).

Thr211 could be exploited with complementary polar atoms on the inhibitor; for example, the dihydrofuranyl derivative of **2** showed >25-fold selectivity for Akt1 over PKA while maintaining druglike properties.⁷ Inhibition by a series of spirochromane compounds has also revealed that PKA inhibition is much more dependent on the nature of the hinge-binding motif than Akt inhibition,¹⁴ again pointing to utility of this region of the Akt active site for generating selectivity. On the basis of these observations and a desire to further improve the selectivity profile of **2**, we decided to pursue additional changes to the hinge-binding motif designed to take advantage of these key insights. In previous analyses of the structure–activity relationship (SAR) for the amino amide portion of pyrrolopyrimidine and dihydrothienopyrimidine compounds, 4-chlorophenyl with an isopropylamine substituent afforded excellent potency, with

reasonable animal pharmacokinetics (PK).^{6,7} Thus, these features were maintained during our initial exploration of the hinge-binding motif.

From our previous efforts, methyl substitution at the 5- and 6-positions of the pyrrolopyrimidine core yielded a modest increase in selectivity over PKA.⁶ Coupled with the selectivity data of the dihydrothienopyrimidine core, we targeted the dihydrocyclopentapyrimidine core as it afforded a better platform to explore additional substitution around the saturated ring. The first of these analogues prepared (Figure 1, **3**) maintained the overall substitution pattern of **2** and proved to be potent, with Akt1 IC_{50} = 6 nM, Akt2 IC_{50} = 12 nM, Akt3 IC_{50} = 5 nM, LNCaP cell p-PRAS40 IC_{50} = 287 nM, and 6-fold selectivity over PKA (PKA IC_{50} = 33 nM). Screening of **3** against a broad panel of 225 kinases found the compound displayed potent inhibition against only 5 additional kinases (>90% inhibition at 1 μ M versus PRKG1 α , PRKG1 β , p70S6K, MSK1, and MSK2) and moderate potency against 14 kinases (>50% inhibition at 1 μ M) and thus appeared to be reasonably selective.¹⁵ Permeability of **3** was high, as measured in a Caco-2 assay: 13.2×10^{-6} cm/s (apical to basolateral, A to B) and 19.2×10^{-6} cm/s for the reverse direction (basolateral to apical, B to A). The compound also displayed a high predicted free fraction with 51% human plasma protein binding. Unfortunately, **3** possessed a rapid in vitro clearance in human hepatocytes (15 mL/min/kg). Given the excellent selectivity, potency, and permeability properties of **3**, it represented a good starting point for further optimization efforts.

From inspection of the X-ray structure of a related dihydrothienopyrimidine inhibitor bound to Akt1, we reasoned that, in the absence of significant changes in the enzyme structure, only relatively small substituents would be tolerated at the 5- and 7-positions of the analogous dihydrocyclopentapyrimidine core (Figure 2). Moreover, due to the proximity of protein atoms, there is more space available above the plane of the bicycle in the 5-position and below the plane of the bicycle in the 7-position. The environment above the plane of the bicycle is

Table 1. Development of the Dihydrocyclopentapyrimidine Core SAR

compd	R ¹	R ²	Akt1 inhibition, IC_{50} ^a nM	Akt2 inhibition, IC_{50} ^a nM	Akt3 inhibition, IC_{50} ^a nM	Akt p-PRAS40 LNCaP IC_{50} ^a nM	PKA inhibition, IC_{50} ^a nM
3	CH ₃	H	6 ± 2	12 ± 4	5 ± 3	287 ± 18	33 ± 9
25	dimethyl	H	>2000	>2000	>2000	ND	>2000
26	vinyl	H	2 ± 1	6 ± 2	1 ± 0	176 ± 31	10 ± 3
33	CH ₂ F	H	3 ± 1	6 ± 2	5 ± 2	123 ± 32	35 ± 12
27	CH ₂ OH	H	81 ± 40	356 ± 53	83 ± 26	846 ± 202	957 ± 332
28	CH ₃	(R)-OH	5 ± 7	18 ± 10	8 ± 9	157 ± 30	3100 ± 705
29	CH ₃	(S)-OH	68 ± 38	249 ± 11	73 ± 27	740 ± 53	1552 ± 455
30	CH ₃	(R)-F	4 ± 2	14 ± 3	10 ± 2	152 ± 31	17 ± 4
31	CH ₃	(S)-F	12 ± 4	35 ± 13	23 ± 5	901 ± 272	541 ± 179
32	CH ₃	diF	1169 ± 487	4177 ± 879	4160 ± 1466	8548 ± 550	>10000

^aValues are means of three or more experiments, and the standard deviation is given. ND = not determined.

largely lipophilic (side chains of Ala177, Val164, Phe225, and Met227), while below the plane it is more hydrophilic (side chains of Thr211 and Thr291) and includes a water molecule coordinated by the backbone and side chain of Glu228. Interestingly, no water molecules are seen proximal to this site in 64 publicly available crystal structures of PKA (multiple inhibitor classes bound and with the majority of the crystals diffracting to better than 2.5 Å) except in cases where Val123 of PKA has been mutated to alanine (equivalent to Ala230 in Akt1), presumably because the increased hydrophobic bulk of valine makes this site unfavorable to water. We note that, in an aligned set of 470 human kinase sequences, only 5% have an alanine corresponding to Ala230 of Akt1, only 11% have a threonine corresponding to Thr211, and only Akt has both. Thus, hydrophilic ligand substituents in the vicinity of Thr211 and the water molecule would be expected to improve selectivity over not only PKA, but also most other kinases.

Polarity at the 5-position of the dihydrocyclopentapyrimidine core (compound 27) did not improve the selectivity and resulted in a loss of potency. Increasing the size of the C5 substituent with hydrophobic groups (26, 33) tended to increase the potency slightly, but afforded no increase in selectivity over PKA. Note that disubstitution at C5 (25) resulted in a significant decrease in potency, which is consistent with the narrow nature of both the Akt and PKA active sites. One particularly interesting finding that emerged from substitution on the core is the profile of the *cis* configuration (Table 1, compounds 29 and 31) relative to the corresponding *trans* analogues. From this comparison, the *cis* substitution for both the fluoro and hydroxy substituents produces an equivalent profile, with high potency against Akt1 and much lower potency against PKA. However, for the *trans* configuration (compounds 28 and 30), the profile diverges dramatically with over a 182-fold separation in PKA activities between the two analogues. The (*R*)-F substituent of 30 is small enough to fit within the cavity near the hinge of PKA; however, this is clearly not the case for the equivalent hydroxy substitution as both the size and polarity of the substituent lead to a significant loss of PKA activity. Interestingly, even though both the *R* and *S* configurations of both the fluoro and hydroxy groups at C7 are potent against Akt, the difluoro analogue (compound 32) was poorly tolerated. The C7-(*R*)-hydroxyl combined with the C5-(*R*)-methyl substitution (Table 1, compound 28) gave ca. 620-fold selectivity versus PKA and afforded good cell potency. Testing against a broad panel of 230 kinases, 28 only inhibited 3 kinases by >70% at 1 μM concentration (PRKG1α, PRKG1β, and p70S6K, with subsequent IC₅₀ values determined to be 98, 69, and 860 nM, respectively).¹⁵ From our perspective, the dihydrocyclopentapyrimidinol core had the desired pan-AKT potency profile and achieved the level of selectivity we felt would ensure a wide safety margin on the basis of our prior efforts.

The binding mode of the 6,7-dihydro-5H-cyclopenta[*d*]pyrimidine core was confirmed by crystallography: the crystal structure of 28 shows that the pyrimidine ring interacts via a hydrogen bond to the amide NH of Ala230 (the N–N distance is 2.97 Å), illustrated in Figure 3. The hydroxyl donates a hydrogen bond to the backbone carbonyl of Glu228 (the O–O distance is 2.66 Å). The isopropylamine side chain interacts in the carbonyl-rich region with the carboxylate side chains of Glu234 (2.96 Å) and Glu278 (2.75 Å). The 4-chlorophenyl group occupies a small hydrophobic pocket under the P-loop that is formed when Phe161 is displaced toward the C-helix. As noted above, one of the key differences we targeted between Akt and PKA, or ROCK1, is the presence of Ala230 (Akt1) in the hinge. The small

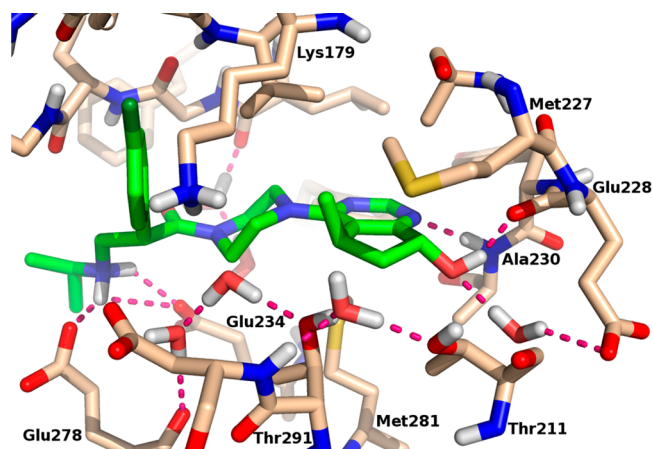


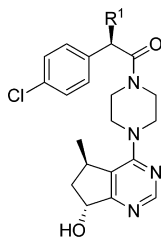
Figure 3. X-ray structure of 28 bound to Akt1, solved at 2.0 Å resolution. Hydrogen atoms added for clarity (PDB code 4EKL).¹⁶

side chain of Ala230 in Akt1 creates a pocket that enables substitution of the dihydrocyclopentapyrimidine core with various groups that afford a high degree of selectivity.

In the previous dihydrothieno- and dihydrofuro-pyrimidine series, metabolism studies identified that amine dealkylation was the major metabolic reaction.⁷ On the basis of similar metabolite identification studies, *N*-dealkylation and oxidation of the core hydroxyl substituent to form the corresponding ketone were the primary routes of metabolism of 28 *in vitro*. The stability, assessed by predicted *in vitro* clearance in human hepatocytes for 28, was 8 mL/min/kg. Given the nature of the amine metabolism, we sought to synthesize analogues with varying degrees of polarity, size, and basicity in an effort to reduce the oxidative loss of the isopropyl group, illustrated in Table 2.

As we observed in the dihydrothienopyrimidine series of compounds,⁷ the secondary amines tended to possess better cell potency relative to the primary amines (e.g., 34 vs 35), likely due to reduced permeability of the latter. The stability in human hepatocytes for 35 decreased significantly (predicted clearance of 11 mL/min/kg). Interestingly, inhibition of PKA does not change for the primary amines, giving rise to a reduced selectivity vs Akt1 for these compounds. Akt1 inhibition is tolerant of many small aliphatic amine substitutions (35–38), while predicted clearance ranged from 9 to 14 mL/min/kg in human hepatocytes for these compounds. Similarly, the tertiary amine analogue of 28 led to only a slight degradation of potency and selectivity (42); however, the predicted clearance increased to 11 mL/min/kg. Larger cyclic aliphatic substitutions of the amine are also well tolerated, with the enzyme potency, cell-based activity, and PKA selectivity all within ca. 5-fold of those of 28 (41, 44, 45, and 46). Constraining the amine also had little effect on inhibition of Akt (47 and 48), although in the case of the pyrrolidine analogue (43) there was a degradation in PKA selectivity. Compound 43 did demonstrate improved stability (clearance in human hepatocytes, 3 mL/min/kg). Likewise, polar additions to the amine chain (39) produced lower clearance compounds (3 mL/min/kg); however, this came at the expense of PKA selectivity. The expected binding mode of these compounds has the amine situated at the lip of the ATP pocket such that these larger substitutions can project into the solvent, thus providing a potential mechanism to alter the physicochemical properties of the inhibitors without significantly compromising the potency. However, the basicity of the amine is an important driver of potency; reducing the p*K_a* below 6.5 led to an 8-fold drop in cell

Table 2. Development of the Amine SAR



Compound	R ¹	Akt1 Inhibition IC ₅₀ , nM ^a	Akt2 Inhibition IC ₅₀ , nM ^a	Akt3 Inhibition IC ₅₀ , nM ^a	Akt p-PRAS40 LNCaP IC ₅₀ , nM ^a	PKA Inhibition IC ₅₀ , nM ^a	calculated pK _a ^b
34		24 ± 10	66 ± 13	45 ± 12	1454 ± 68	700 ± 167	9.7
35		5 ± 0	12 ± 3	5 ± 2	179 ± 37	777 ± 255	9.2
36		12 ± 7	33 ± 8	21 ± 8	1296 ± 356	1315 ± 354	6.2
37		902 ± 93	2005 ± 397	798 ± 92	ND	> 10000	2.9
38		8 ± 5	17 ± 2	13 ± 4	384 ± 61	1004 ± 251	9.1
39		2 ± 1	4 ± 2	3 ± 1	75 ± 15	293 ± 105	9.2
40		6 ± 2	11 ± 3	10 ± 2	196 ± 51	1196 ± 378	6.7
41		9 ± 3	18 ± 3	7 ± 3	367 ± 40	1277 ± 350	9.9
42		18 ± 10	31 ± 11	28 ± 10	139 ± 19	2136 ± 514	9.8
43		3 ± 1	6 ± 2	5 ± 1	241 ± 12	271 ± 81	9.5
44		5 ± 3	15 ± 4	5 ± 2	184 ± 34	654 ± 247	10.1
45		5 ± 2	10 ± 3	4 ± 1	132 ± 30	662 ± 162	9.1
46		3 ± 1	6 ± 3	4 ± 1	102 ± 26	436 ± 160	9.0
47		9 ± 5	22 ± 7	12 ± 2	530 ± 71	1595 ± 470	9.5
48		12 ± 5	29 ± 5	26 ± 6	855 ± 179	1364 ± 398	6.3

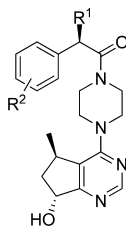
^aValues are means of three or more experiments, and the standard deviation is given. ND = not determined. ^bpK_a values were calculated using a custom pK_a model implemented in the MoKa software, version 1.1, from Molecular Discovery Ltd.¹⁷

potency (36), while reducing the pK_a below 3.0 led to a 180-fold decrease in enzyme activity (37). Although some of the analogues in Table 2 did show modest improvements in potency, none had dramatic improvements in metabolic stability while retaining cellular potency and selectivity.

Finally, we explored the effect of amine substitution in conjunction with aromatic ring changes to probe the contacts

with the underside of the P-loop of Akt1 (Table 3). Replacing the 4-Cl with a 4-CF₃ group improves the potency in the context of the primary amine (comparing 49 and 34), although selectivity over PKA is still only moderate. Addition of a 3-F group to the secondary amines gives analogues with similar potency and selectivity over PKA (compare 50 to 28 or 54 to 44). Combining the 3-F with the 4-CF₃ substitution led to a 3–4-fold

Table 3. Development of the Cyclopentapyrimidinol Core SAR



Compound	R ¹	R ²	Akt1 Inhibition IC ₅₀ , nM ^a	Akt2 Inhibition IC ₅₀ , nM ^a	Akt3 Inhibition IC ₅₀ , nM ^a	Akt p-PRAS40 LNCaP IC ₅₀ , nM ^a	PKA Inhibition IC ₅₀ , nM ^a
49		4-CF ₃	12 ± 5	30 ± 7	27 ± 8	603 ± 127	418 ± 99
50		3-F,4-Cl	3 ± 2	17 ± 10	7 ± 3	234 ± 23	490 ± 194
51		3-F,4-CF ₃	3 ± 1	5 ± 1	3 ± 1	92 ± 16	153 ± 45
52		3-F,4-CF ₃	6 ± 1	6 ± 1	2 ± 1	47 ± 11	75 ± 5
53		3-F,4-CF ₃	3 ± 1	3 ± 1	2 ± 1	65 ± 1	103 ± 41
54		3-F,4-Cl	12 ± 6	24 ± 7	12 ± 5	139 ± 33	556 ± 207

^aValues are means of three or more experiments, and the standard deviation is given.

improvement in enzyme and cellular potency; however, this substitution pattern reduces the selectivity ratio of PKA/Akt1 to be ca. 35-fold or less (e.g., comparing 53 to 35 or 52 to 39). While compounds 52 and 53 did show improved cellular potency, the predicted stability (clearance of 7 and 13 mL/min/kg in human hepatocytes, respectively) decreased, presumably due to the increased lipophilicity of the 3-F-4-CF₃ substitution.

From our exploration of the structure–activity relationship around the dihydrocyclopentapyrimidinol core, 28 remained one of the most selective compounds we have discovered, while maintaining good potency against all three Akt isoforms and high potency in cell-based assays. None of the analogues present in Tables 2 and 3 offered any significant improvement of in vitro stability and selectivity over 28, so 28 was advanced into additional profiling. As with the corresponding dihydrocyclopentapyrimidine (3), 28 is also predicted to have a high free-drug fraction in plasma for both human and preclinical species with 39% human plasma protein binding and 44% measured in monkey and 56% in mouse. Consistent with the plasma protein binding results, the solubility of 28 was very high, being greater than 10 mg/mL at three pH values (1.2, 6.5, and 7.4). 28 also possessed low to moderate predicted in vitro clearance in human, monkey, and mouse hepatocytes (8, 27, and 8 mL/min/kg, respectively).

In keeping with observations with other ATP-competitive Akt inhibitors,^{18–21} there is an increase of phosphorylated Akt levels when cells are treated with 28.²² However, the data in Table 1 clearly show that 28 potently inhibits Akt signaling in LNCaP cells (which have a high basal pAkt level due to loss of PTEN), indicating that the increased level of phosphorylated Akt is not functionally active in these cells.²² Additionally, 28 has a potent antiproliferative effect on this cell line with an IC₅₀ of 95 ± 16

nM. We extended this analysis to other cell lines, including PC3, MCF7-neo/HER2, and BT474M1. In all three lines, 28 was able to inhibit overall viability with IC₅₀ values in the range of 1–4 μM. More detailed analysis demonstrated that 28 induces a dose-dependent block of the cell-cycle progression at the G1 phase and a dose- and time-dependent increase in apoptosis and necrosis in MCF7-neo/HER2 and BT474M1 cells (data not shown; a more complete discussion of these studies will be presented elsewhere). All four of the cell lines tested have elevated levels of basal Akt signaling due to loss of PTEN (PC3 and LNCaP), mutation of PI3Kα (MCF7-neo/HER2), or overexpression of Her2 (MCF7-neo/HER2 and BT474M1). Thus, the inhibition of signaling and reduced viability suggest that 28 will be useful in controlling human cancers in which PI3K/Akt signaling is overly active. 28 was able to inhibit phosphorylation of PRAS40 in all four of these cell lines with IC₅₀ values comparable to that observed in LNCaP cells (ca. 200 nM, data not shown).

PK studies of 28 in nu/nu mice were performed to support pharmacodynamic and efficacy studies. The animals were given a single per os (po) dose of 28 at 12.5 and 50 mg/kg (0.5% methylcellulose with 0.2% polysorbate 80 (MCT) dose solutions). Systemic exposure increased in a more than dose-proportional fashion with increasing dose, leading to good exposures. Plasma concentrations were at or above 200 nM for the 12.5 and 50 mg/kg dose groups, respectively, within 1 h of drug administration. With the 50 mg/kg po dose, plasma concentrations were approximately 7.4 μM at 1 h postdose and 0.5 μM at 9 h postdose; the concentration of 28 was above 200 nM for approximately 9 h (this concentration is higher than the cellular IC₅₀ for p-PRAS40 knockdown in LNCaP cells; see Table 1). PK studies performed in rat and monkey also gave

acceptable oral exposures (data not shown), suggesting that reasonable oral exposures in humans can be achieved.

A pharmacodynamic (PD) and PK study was performed in nu/nu mice bearing subcutaneous PC3 prostate tumors to correlate plasma drug levels of **28** with PD changes in the tumors. Following administration of a single po dose, plasma and tumor samples were collected from the animals between 1 and 24 h for PK and PD analysis, respectively. As described above, robust Akt pathway inhibition with **28** was determined in vitro on the basis of the suppression of p-PRAS40. Therefore, this PD marker relative to the total protein level was also evaluated in vivo. Within 3 h of drug administration, there was a dose-dependent decrease in the ratio of p-PRAS40 to tPRAS40 compared with vehicle controls, with a >95% reduction achieved at 100 mg/kg (Figure 4A). At 8 h postdose, plasma levels of **28** of >2.6 μM

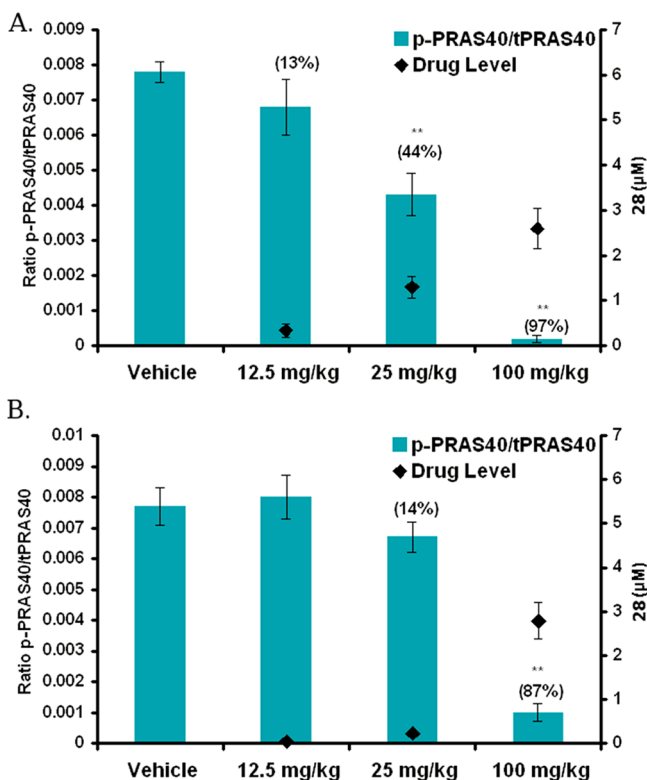


Figure 4. PK/PD of **28** in PC3 prostate tumors. Tumor ratios of p-PRAS40 to total PRAS40 (tPRAS40) were determined in female nude mice bearing PC3 prostate tumor xenografts (average of five animals \pm SEM). Plasma concentrations of **28** were also measured. Samples were collected 3 h (A) or 8 h (B) following administration of 12.5, 25, and 100 mg/kg doses (free base equivalents formulated in 0.5% methylcellulose/0.2% Tween-80). The inhibition (%) of p-PRAS40/tPRAS40 is based on comparison to the vehicle control and stated in parentheses. Average drug levels \pm SEM (μM) of **28** were determined by analysis of plasma from five animals. Two asterisks indicate $p < 0.001$, determined by Student's t test to find differences in biomarker effects for dosing groups vs the vehicle control.

were maintained with 100 mg/kg, and this correlated with an 87% inhibition of p-PRAS40/tPRAS40 (Figure 4B). Furthermore, pS6RP is also significantly reduced under these conditions (data not shown). These data demonstrate that **28** is able to significantly inhibit the Akt pathway in PC3 prostate tumors for at least 8 h postdose at 100 mg/kg.

Multiple doses of **28** were also administered daily (qd) or twice daily (bid) in nude mice bearing PC3 prostate cancer

xenografts. Daily doses ranged from 25 to 100 mg/kg. Even the lowest dose resulted in statistically significant tumor growth inhibition (49%, $p < 0.009$) when administered qd for 11 days (Figure 5); hence, the minimum efficacious dose was determined

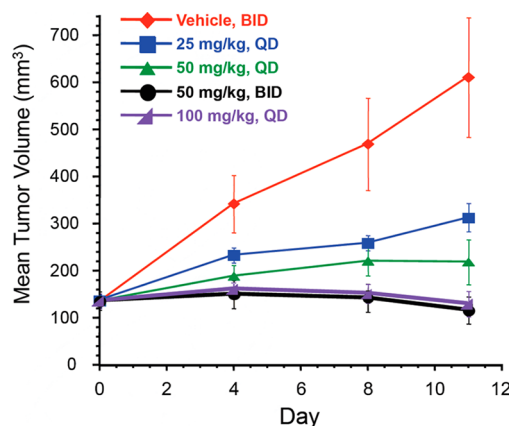


Figure 5. Effect of qd and bid oral dosing of **28** on PC3 prostate tumors (mean tumor volume in cubic millimeters \pm SEM). Dose levels are expressed as free-base equivalents prepared in vehicle (0.5% methylcellulose/0.2% Tween-80).

to be 25 mg/kg. The maximum tumor growth inhibition was obtained with qd dosing of **28** for 11 days at 100 mg/kg (79%, $p < 0.0001$). In addition, half-maximal doses of **28** (50 mg/kg) given orally bid resulted in a nearly equivalent tumor growth inhibition of 81% when compared with qd dosing of 100 mg/kg (Figure 5, not statistically different). Thus, **28** is efficacious against human PC3 prostate cancer xenografts in vivo when dosed orally either qd or bid. Overall body weight loss, including the vehicle control group, was observed in all groups tested due to the cachectic nature of this model.²³ Doses of 0–100 mg/kg **28** qd caused less than 10% mean body weight loss, whereas doses of 150 mg/kg qd caused $\geq 20\%$ loss of original body weight after eight doses, and the mice had to be euthanized before the completion of the study (data not shown).

CONCLUSIONS

We have described the discovery of **28**, and related compounds, for the treatment of human tumors. The novel ATP-competitive, selective Akt inhibitors were optimized via structure-based design to target unique features of the Akt ATP binding cleft, resulting in exquisitely selective and potent inhibitors. In the specific case of **28**, this strategy led to good selectivity in a 230-enzyme kinase panel. Extensive in vitro profiling has shown that human cancer cell lines in which the PI3K/Akt pathway is upregulated are sensitive to inhibition by **28**; in spite of an increase in pAkt levels, downstream signaling in this pathway is inhibited by **28**, providing a mechanistic explanation of the antiproliferative and antisurvival effects. The in vitro effects are recapitulated in the in vivo models, wherein we see good oral exposures, a significant inhibition of Akt signaling following a single dose of **28**, and a robust inhibition of tumor growth following repeated qd or bid oral dosing in a mouse xenograft model of PI3K/Akt-driven cancer. Given all of these data, **28** is currently being investigated in human clinic trials for the treatment of cancers driven by aberrant PI3K/Akt signaling.

■ EXPERIMENTAL SECTION

Enzymatic Assays. The assay for the determination of Akt1/2/3 and PKA kinase activity employs the IMAP fluorescence polarization (FP) phosphorylation detection reagent (IMAP Screening Express Kit, catalog no. R8073, Molecular Devices, Sunnyvale, CA) to detect fluorescently labeled peptide substrates that have been phosphorylated by the respective kinases. The Akt enzymes employed in these studies consisted of recombinant baculovirus expressed, amino-terminal, polyhistidine-tagged, full-length, wild-type human forms (GenBank accession numbers M63167, NP_001617, and NP_005456) and were obtained from Millipore (Akt1, catalog no. 14 276, lot no. D8MN034U; Dundee, Scotland) or Invitrogen (Akt2, catalog no. PV3184, lot no. 28770P; Akt3, catalog no. PV3185, lot no. 28771K; Madison, WI). The PKA enzyme employed in these studies consisted of the recombinant untagged human isolated catalytic subunit of PKA (GenBank accession number X07767) expressed in *Escherichia coli* obtained from Invitrogen (catalog no. 14-440, lot no. 26698U). Inhibitor, enzyme (9 nM Akt1 or 100 pM PKA), and substrate (100 nM Crosstide, catalog no. R7110, Molecular Devices) were incubated with 5 μ M ATP in assay buffer (10 mM Tris-HCl (pH 7.2), 10 mM MgCl₂, 0.1% BSA (w/v), final DMSO 2% (v/v)) for 60 min at ambient temperature in a 5 μ L reaction volume. Reactions were initiated by addition of enzyme + peptide substrate to ATP solutions. IMAP binding reagent (15 μ L) was added to terminate the reaction, and the stopped reactions were incubated for a minimum of 30 min at room temperature (rt).

Cellular Assays. Phosphorylation of PRAS40 at Thr246 was measured in situ in LNCaP cells (American Type Culture Collection, catalog no. CRL-1740). The cells were plated in 96-well plates (Grenier, catalog no. 655946) at a density of 20 000 cells/well and incubated for 16–24 h at 37 °C and 5% CO₂. The cells were treated with 0–25 μ M inhibitor for 1.5 h at 37 °C. Medium above the cells was removed, and each well was supplemented with fixation solution (3.7% (v/v) formaldehyde in phosphate-buffered saline (PBS)) for 20 min at rt. The cells were permeabilized with a 10 min exposure to 100% methanol (–20 °C) and subsequently rehydrated in PBS and blocked in blocking buffer (catalog no. 927-40000, LI-COR Inc., Lincoln, NE) for 60 min at rt. A primary antibody solution consisting of an antibody specific for Thr246-phosphorylated PRAS40 (rabbit polyclonal antibody, 1:500 dilution, catalog no. AS1011, Calbiochem, San Diego, CA) and a signal-normalizing antibody against glyceraldehyde 3-phosphate dehydrogenase (GAPDH; mouse monoclonal, 1 μ g/mL final concentration, catalog no. RDI-TRK5-6C5, Fitzgerald Industries Inc., Concord, MA) in blocking buffer was applied to each of the wells and incubated overnight at 4 °C. The wells were then washed with PBS containing 0.05% (v/v) Tween-20, treated with a secondary antibody solution containing fluorophore-conjugated antibodies specific for rabbit (Alexa680 fluorophore-conjugated goat antirabbit immunoglobulin G (IgG), catalog no. AS21109, Invitrogen) and mouse IgG (IRDye800 fluorophore-conjugated goat antimouse IgG, catalog no. 610-132-121, Rockland Inc., Gilbertsville, PA), and incubated for 1 h at rt. The wells were washed in PBS with 0.05% (v/v) Tween-20 and then imaged and quantified on an LI-COR Aeries imager (LI-COR Inc.). The phospho-PRAS40 signal was normalized to the GAPDH signal to control for well-to-well variation in cell number.

Inhibition of cellular viability was measured in LNCaP cells (American Type Culture Collection, catalog no. CRL-1740) plated in black, clear-bottomed 96-well plates (Grenier, catalog no. 655946) at a density of 5000 cells/well and subsequently treated with 0–10 μ M **28** for 72 h at 37 °C and 5% CO₂. The extent of cell proliferation was determined by measuring the reduction of resazurin to resorufin as described in the manufacturer's protocol (CellTiterBlue Cell Viability Determination Kit, catalog no. G8082, Promega, Madison, WI) using an excitation wavelength of 560 nm and an emission wavelength of 590 nm. Dose–response curves were generated using the four-parameter logistic model, and 50% inhibitory concentration (IC₅₀) values were determined from these curve fits.

Inhibition of cellular proliferation was measured in PC3-NCL, MCF7-neo/HER2-neo/Her2, and BT474M1 cells plated in black, clear-bottomed 384-well plates (catalog no. 353962, Becton Dickinson,

Franklin Lakes, NJ) at a density of 1500 cells/well and incubated overnight to 1.5 days at 37 °C and 5% CO₂. Serial dilutions of inhibitor were added to the cells, which were then incubated for another 96 h. Cell viability was determined by measuring the cellular ATP levels as described in the manufacturer's protocol (CellTiter-Glo Luminescent Cell Viability Assay Kit, catalog no. G7573, Promega, Madison, WI). Dose–response curves were generated using the four-parameter logistic model, and 50% inhibitory concentration (IC₅₀) values were determined from these curve fits.

In Vivo Efficacy and PK/PD. For in vivo tumor xenograft studies, female nu/nu (nude) mice were inoculated subcutaneously in the right hind flank with PC3 cells suspended in Hank's balanced salt solution (HBSS). When tumors reached a mean volume of 150 mm³, the animals were size matched and distributed into treatment groups consisting of 10 animals/group. Tumor volume was calculated as follows: tumor size (mm³) = (longer measurement \times (shorter measurement)²) \times 0.5. Following data analysis, *p* values were determined using Dunnett's *t* test with JMP statistical software, version 7.0 (SAS Institute). Mouse body weights were recorded twice weekly using an Adventura Pro AV812 scale (Ohaus Corp.). Mice were promptly euthanized when the tumor volume exceeded 2000 mm³ or if body weight loss was \geq 20% of the starting weight per IACUC protocol guidelines.

For PK/PD studies, blood and tumor samples were collected at 1, 3, 8, and 24 h after a single dose of **28** from PC3 tumor bearing mice. Blood samples (approximately 800 μ L) were collected from each animal at the scheduled sample collection time by terminal cardiac puncture into tubes containing K₂EDTA as an anticoagulant and centrifuged at 1500–2000g to isolate plasma. The concentration of **28** in each plasma sample was determined by a nonvalidated LC/MS/MS assay in the DMPK Bioanalytical Department at Genentech. The assay lower limit of quantitation (LLOQ) was 0.005 μ M. Tumor samples were dissociated in Tris lysis buffer containing 150 mM NaCl, 20 mM Tris (pH 7.5), 1 mM EDTA, 1 mM EGTA, and 1% Triton X-100 (Meso Scale Discovery; Gaithersburg, MD). Protein concentrations were determined using the BCA Protein Assay Kit (Pierce, Rockford, IL). The Invitrogen (Camarillo, CA) human enzyme-linked immunosorbent assay (ELISA) kits were used to determine the levels of total PRAS40 and PRAS40 phosphorylated at Thr246 (p-PRAS40). The assay quantifies protein levels on the basis of measurements of absorbance. The colored product is directly proportional to the concentration of p-PRAS40 and tPRAS40 present in the specimen. The Meso Scale Discovery Multi-Spot Biomarker Detection System (Meso Scale Discovery) was used to determine the levels of total S6RP and S6RP phosphorylated at Ser235/236 (pS6RP). These assays quantify protein levels on the basis of measurements of electrochemiluminescence intensity. Levels of phosphorylated protein were normalized to total protein levels in **28**-treated tumors and compared to the vehicle control.

Chemistry. All reaction reagents and solvents (anhydrous grade) were purchased and used without further purification. ¹H NMR spectra were recorded on a Varian INOVA 400 instrument. Chemical shifts are reported in parts per million relative to an internal standard of TMS in CDCl₃ or DMSO-*d*₆. HPLC analysis was conducted according to methods A–E, with the retention time (*t*_R) expressed in minutes at UV detection of 254 nm. Chromatography was performed on a Varian Prostar with a YMC ODS-C18-AQ column (4.6 \times 50 mm, 3 μ m) at 40 °C with a flow rate of 2.0 mL/min. Mobile phase A was 10 mM NH₄OAc in water with 1% isopropyl alcohol. Mobile phase B was 10 mM NH₄OAc, 1% H₂O, and isopropyl alcohol in acetonitrile. HPLC method A: The gradient was 5% B to 95% B in 5 min. HPLC method B: The gradient was 0% B to 95% B in 5 min. HPLC method C: Chromatography was performed on an Agilent HPLC instrument with a Zorbax SB C18 column (4.6 \times 50 mm, 3 μ m) with a flow rate of 2.0 mL/min. Mobile phase A was 0.1% TFA in water, and mobile phase B was 0.075% TFA in acetonitrile. The gradient was 5% B to 95% B in 9 min. HPLC method D: Chromatography was performed on an Agilent 6140 HPLC instrument with a Zorbax SB C18 column (2.1 \times 30 mm, 1.8 μ m) at 40 °C with a flow rate of 0.4 mL/min. Mobile phase A was 0.05% TFA in water, and mobile phase B was 0.05% TFA in acetonitrile. The gradient was 3% B to 95% B in 8.5 min. HPLC method E: Chromatography was performed on an Agilent 6140 HPLC instrument

with a Zorbax SB C18 column (3.0 × 100 mm, 3.5 μm) at 40 °C with a flow rate of 0.7 mL/min. Mobile phase A was 0.05% TFA in water, and mobile phase B was 0.05% TFA in acetonitrile. The gradient was 2% B to 98% B in 25.5 min. Mass spectral analysis was conducted on a Thermo Separation Products (TSP) HPLC or Waters Micromass ZQ instrument.

(2R)-Ethyl 2-Methyl-5-oxocyclopentanecarboxylate (5a). To a 5 L round-bottom flask were added (R)-pulegone (600.0 g, 3.94 mol), anhydrous NaHCO₃ (165.0 g, 1.97 mol), and ether (2.0 L). The mixture was cooled to 0 °C using an ice bath, and bromine (206.0 mL, 4.02 mol) was added dropwise over 1 h. The reaction was allowed to stir for an additional 30 min after bromine addition was complete, and the mixture was filtered to give filtrate A. To a separate 12 L round-bottom reactor equipped with a mechanical stirrer and a thermocouple were charged 21% NaOEt (3.2 L, 8.7 mol) and EtOH (2.0 L). This reaction mixture was cooled to 0 °C, and filtrate A was added dropwise at a rate which maintained an internal temperature below 40 °C. *Caution: Addition is exothermic, and adequate cooling is required!* After complete addition of filtrate A, the reaction was allowed to warm to rt. The reaction was quenched by the addition of 1 N HCl (1.0 L) and water (1.5 L), followed by the addition of methyl *tert*-butyl ether (MTBE; 1.0 L). The organic layer was separated and the aqueous phase extracted with MTBE (3 × 1.5 L). The combined organic layers were concentrated to give a brown oil. To a second 12 L round-bottom reactor equipped with a mechanical stirrer were charged semicarbazide hydrochloride (300.0 g, 2.6 mol), NaOAc (300.0 g, 3.6 mol), and water (3.0 L). The crude oil from above was added slowly as a solution in ethanol (1.5 L). The mixture was then refluxed for 3 h and stirred at rt overnight. The mixture was treated with water (1.0 L) and MTBE (1.0 L). The organic layer was separated, and the aqueous phase was extracted with MTBE (3 × 1.5 L). The combined organic layer was washed with brine and concentrated to give a brown oil. The oil was distilled under vacuum to give (2R)-ethyl 2-methyl-5-propan-2-ylidenecyclopentanecarboxylate (497 g, 64% yield) collected at 73–76 °C at 0.5 mm as a clear oil: ¹H NMR (CDCl₃, 400 MHz) δ 4.17–4.07 (m, 2H), 3.39 (d, J = 8.0 Hz, 0.5 H), 2.93 (d, J = 6.0 Hz, 0.5 H), 2.48–2.15 (m, 3 H), 2.03–1.98 (m, 1H), 1.79–1.72 (m, 1H), 1.65–1.59 (m, 6H), 1.25 (t, J = 8.0 Hz, 3H), 1.03 (dd, J = 12.0, 6.8 Hz, 3H).

A solution of (2R)-ethyl 2-methyl-5-propan-2-ylidenecyclopentanecarboxylate (220.0 g, 1.1 mmol) in EtOAc (1.0 L) was cooled to –78 °C using a dry ice/2-propanol bath. Ozone was bubbled into the reaction mixture until it turned purple in color. At this point ozone generation was stopped, and the reaction mixture was removed from the dry ice bath. Nitrogen was bubbled through the reaction solution until it turned yellow. The reaction was concentrated and the resulting residue dissolved in glacial acetic acid (200 mL). The solution was cooled to 0 °C, and zinc dust (113.0 g, 1.7 mol) was added in small portions over a 30 min period. The reaction was allowed to stir for 1.5 h, at which point the reaction mixture was filtered through Celite. The resulting solution was concentrated in vacuo to remove acetic acid, and the residue was diluted with MTBE (500 mL). The mixture was neutralized to pH 7.0 by careful addition of aqueous 6 N NaOH. The organic layer was separated, and the aqueous layer was extracted with MTBE (2 × 250 mL). The combined organics were washed with brine, dried with solid MgSO₄, and concentrated by rotary evaporation to give a dark brown liquid. This liquid was passed through a plug of silica gel eluting with a small amount of MTBE. The combined filtrate was again concentrated by rotary evaporation to give the desired (2R)-ethyl 2-methyl-5-oxocyclopentanecarboxylate (180.1 g, 94% yield) as a light brown liquid which was used without any further purification: ¹H NMR (CDCl₃, 400 MHz) δ 4.21 (q, J = 6.4 Hz, 2H), 2.75 (d, J = 11.2 Hz, 1H), 2.64–2.56 (m, 1H), 2.46–2.30 (m, 2H), 2.24–2.16 (m, 1H), 1.53–1.42 (m, 1H), 1.29 (t, J = 6.4 Hz, 3H), 1.19 (d, J = 6.4 Hz, 3H).

General Procedure for Formation of the Cyclopenta[d]pyrimidine Core: (R)-5-Methyl-6,7-dihydro-5H-cyclopenta[d]pyrimidin-4-ol (6a). To a solution of 5a (150.1 g, 881 mmol) in MeOH (2.0 L) was added NH₄OAc (268.2 g, 3.5 mol). The reaction mixture was stirred overnight and concentrated under reduced pressure. The resulting residue was dissolved in dichloromethane (DCM; 1.0 L) and partitioned with water (2.0 L). The organic layer was separated, and the aqueous layer was extracted with DCM (3 × 750 mL). The combined organics

were washed with brine, dried over solid MgSO₄, and concentrated in vacuo to give the desired (R)-ethyl 2-amino-5-methylcyclopent-1-enecarboxylate (136.2 g, 91% yield) as a brown oil. This material was used without further purification: ¹H NMR (CDCl₃, 400 MHz) δ 5.5 (br s, 2H), 4.22–4.10 (m, 2H), 2.98–2.94 (m, 1H), 2.64–2.55 (m, 1H), 2.37–2.29 (m, 1H), 2.09–1.99 (m, 1H), 1.45–1.38 (m, 1H), 1.28 (t, J = 6.4 Hz, 3H), 1.96 (d, J = 6.4 Hz, 3H); LC/MS APCI (+) *m/z* 170.1 (M + H)⁺.

To a 2 L three-necked magnetically stirred round-bottom reactor equipped with a condenser and thermocouple were added (R)-ethyl 2-amino-5-methylcyclopent-1-enecarboxylate (308.0 g, 1.8 mol), ammonium formate (172.0 g, 2.7 mol), and formamide (504 mL, 12.7 mol). The mixture was heated to an internal temperature of 150 °C for 24 h. *Note: Sublimed ammonium formate could build up in the condenser. Addition of 25 mL of a lower boiling solvent such as *o*-xylene helps keep the condenser clear.* The reaction mixture was cooled and transferred to 2 L single-neck flask, and the excess formamide was removed by distillation under vacuum. Once removal of the formamide was complete, the flask was cooled, and the resulting oil was dissolved in DCM (2.0 L) and washed with brine (3 × 200 mL). The organic layer was dried over Na₂SO₄, filtered, and concentrated by rotary evaporation. The resulting brown oil was dissolved in a small amount of DCM and slowly added to a stirring solution of ether (ca. 5× volume of ether vs DCM), resulting in a brown slurry. The slurry was filtered, and the resulting wet cake was rinsed with ether. The brown filtrate was concentrated by rotary evaporation and dried under high vacuum to give crude (R)-5-methyl-6,7-dihydro-5H-cyclopenta[d]pyrimidin-4-ol (180.1 g, 66% yield). This material was used without further purification: ¹H NMR (CDCl₃, 400 MHz) δ 12.8 (br s, 1H), 8.07 (s, 1H), 3.35–3.29 (m, 1H), 2.98–2.91 (m, 1H), 2.85–2.78 (m, 1H), 2.36–2.26 (m, 1H), 1.71–1.64 (m, 1H), 1.31 (d, J = 6.4 Hz, 3H); LC/MS APCI (+) *m/z* 151.1 (M + H)⁺.

General Procedure for the Incorporation of Boc-Protected Piperazine. (R)-*tert*-Butyl 4-(5-Methyl-6,7-dihydro-5H-cyclopenta[d]pyrimidin-4-yl)piperazine-1-carboxylate (7a). To a solution of (R)-5-methyl-6,7-dihydro-5H-cyclopenta[d]pyrimidin-4-ol (150.1 g, 998 mmol) in 1,2-dichloroethane (DCE; 500 mL) was added POCl₃ (233 mL, 2.5 mol) dropwise. The reaction mixture was heated to reflux for 6 h and concentrated by rotary evaporation. The crude oil was diluted with a small amount of DCM to give a suspension, which was added to a stirring solution of 6 M aqueous NaHCO₃ (more NaHCO₃ was added as needed to keep the solution basic). The organic layer was separated, and the aqueous layer was extracted with DCM (2 × 250 mL). The combined organics were dried over MgSO₄, filtered, and concentrated in vacuo. The crude brown oil was purified by passing through a silica plug eluting with hexanes–EtOAc (4:1) to give the desired (R)-4-chloro-5-methyl-6,7-dihydro-5H-cyclopenta[d]pyrimidine (81.2 g, 48% yield) as a brown liquid: ¹H NMR (CDCl₃, 400 MHz) δ 8.77 (s, 1H), 3.46–3.41 (m, 1H), 3.20–3.11 (m, 1H), 2.98 (ddd, J = 10.2, 6.4, 6.4, 1H), 2.42–2.32 (m, 1H), 1.86–1.78 (m, 1H), 1.34 (d, J = 6.4 Hz, 3H); LC/MS APCI (+) *m/z* 169.3 (M + H)⁺.

A solution of (R)-4-chloro-5-methyl-6,7-dihydro-5H-cyclopenta[d]pyrimidine (73.3 g, 434.7 mmol), *tert*-butyl piperazine-1-carboxylate (85.0 g, 456.4 mmol), and *N,N*-diisopropylethylamine (DIEA; 227.0 mL, 1.30 mol) in 1-BuOH (720 mL) was heated to reflux under a nitrogen atmosphere for 16 h. The reaction mixture was concentrated by rotary evaporation, and the crude residue was purified by silica gel chromatography eluting with hexanes–EtOAc (2:1) to EtOAc to give a brown solid. The solid was recrystallized from heptane to give the desired pure (R)-*tert*-butyl 4-(5-methyl-6,7-dihydro-5H-cyclopenta[d]pyrimidin-4-yl)piperazine-1-carboxylate (112.6 g, 81% yield) as an off-white solid: ¹H NMR (CDCl₃, 400 MHz) δ 8.47 (s, 1H), 3.72–3.68 (m, 2H), 3.57–3.44 (m, 7H), 2.96–2.84 (m, 2H), 2.32–2.26 (m, 1H), 1.72–1.67 (m, 1H), 1.48 (s, 9H), 1.79 (d, J = 7.2 Hz, 3H); LC/MS APCI (+) *m/z* 319.1 (M + H)⁺.

***tert*-Butyl 4-((5R)-7-Acetoxy-5-methyl-6,7-dihydro-5H-cyclopenta[d]pyrimidin-4-yl)piperazine-1-carboxylate (9).** To a 3 L three-necked round-bottom reactor equipped with a mechanical stirrer, nitrogen inlet, and thermocouple at 0 °C containing a mixture of 7a (50.1 g, 157.0 mmol), solid NaHCO₃ (46.2 g, 550.4 mmol), and CHCl₃ (700 mL) was added *m*-chloroperoxybenzoic acid (*m*-CPBA; 45.0 g,

197.2 mmol, 75% by weight) in small portions. After the addition was complete, the reaction mixture was stirred at 0 °C for 10 min and then warmed to rt for 4.5 h. The reaction mixture was cooled to 0 °C, and a solution of Na₂S₂O₃ (49.7 g, 314 mmol) in water (70 mL) was added slowly. After complete addition, the reaction mixture was stirred at 0 °C for 10 min. The pH of the mixture was adjusted by the dropwise addition of Na₂CO₃ (66.6 g, 628.0 mmol) as a solution in water (100 mL). The reaction mixture was stirred for 20 min and then warmed to rt for 10 min. The mixture was diluted with water (200 mL) and partitioned with CHCl₃ (200 mL). The organic layer was separated, and the aqueous layer was extracted with CHCl₃ (2 × 400 mL). The combined organics were washed with saturated Na₂CO₃ (500 mL), dried over Na₂SO₄, filtered through Celite, and concentrated in vacuo to give the crude (R)-4-(4-(*tert*-butoxycarbonyl)piperazin-1-yl)-5-methyl-6,7-dihydro-5H-cyclopenta[*d*]pyrimidine 1-oxide (52.5 g, 100% yield), which was used without purification in the next step: LC/MS APCI (+) *m/z* 335.1 (M + H)⁺.

To a round-bottom reactor containing the (R)-4-(4-(*tert*-butoxycarbonyl)piperazin-1-yl)-5-methyl-6,7-dihydro-5H-cyclopenta[*d*]pyrimidine 1-oxide (42.0 g, 126.0 mmol) was slowly added acetic anhydride (178 mL, 1.8 mol) (*note: mild exotherm*). After complete addition, the reaction mixture was heated to 100 °C and stirred under a nitrogen atmosphere for 2 h. The reaction mixture was cooled to rt and concentrated by rotary evaporation to remove excess acetic anhydride. The resulting residue was dissolved in DCM (1.0 L), and the solution was poured into ice and aqueous saturated Na₂CO₃ (500 mL). The organic layer was separated, and the aqueous layer was extracted with DCM (2 × 200 mL). The combined organic extracts were washed with brine, dried over Na₂SO₄, and concentrated in vacuo. The crude material was passed through a plug of silica gel eluting with hexanes–EtOAc (1:1) to give the desired *tert*-butyl 4-((5*R*)-7-acetoxy-5-methyl-6,7-dihydro-5H-cyclopenta[*d*]pyrimidin-4-yl)piperazine-1-carboxylate (42.0 g, 89% yield) as a brown foam after rotary evaporation: ¹H NMR (CDCl₃, 400 MHz) δ 8.60 (s, 1H), 6.04 (t, *J* = 7.2 Hz, 1H), 3.80–3.76 (m, 2H), 3.74–3.46 (m, 7H), 2.31–2.23 (m, 2H), 2.14 (s, 3H), 1.49 (s, 9H), 1.21 (d, *J* = 7.2 Hz, 3H); LC/MS APCI (+) *m/z* 333.1 (M + H)⁺.

(*R*)-*tert*-Butyl 4-(5-Methyl-7-oxo-6,7-dihydro-5H-cyclopenta[*d*]pyrimidin-4-yl)piperazine-1-carboxylate (**10**). To a solution of the *tert*-butyl 4-((5*R*)-7-acetoxy-5-methyl-6,7-dihydro-5H-cyclopenta[*d*]pyrimidin-4-yl)piperazine-1-carboxylate (16.5 g, 43.8 mmol) in THF (200 mL) was added 3 M LiOH (40 mL, 120 mmol). The reaction mixture was stirred at rt for 16 h and then neutralized with the addition of 2 N HCl (60 mL). The mixture was concentrated by rotary evaporation, and the residue was purified by silica gel chromatography eluting with DCM–MeOH (10:1) to give the desired *tert*-butyl 4-((5*R*)-7-hydroxy-5-methyl-6,7-dihydro-5H-cyclopenta[*d*]pyrimidin-4-yl)piperazine-1-carboxylate (14.5 g, 99% yield) as a clear oil: ¹H NMR (CDCl₃, 400 MHz) δ 8.47 (s, 1H), 3.72–3.68 (m, 2H), 3.57–3.43 (m, 7H), 2.96–2.81 (m, 2H), 2.32–2.26 (m, 1H), 1.73–1.65 (m, 1H), 1.48 (s, 9H), 1.17 (d, *J* = 7.2 Hz, 3H); LC/MS APCI (+) *m/z* 335.2 (M + H)⁺.

To a 1 L three-necked round-bottom reactor containing a solution of oxalyl chloride (21.2 mL, 243.4 mmol) in DCM (150 mL) at –78 °C was added a solution of dimethyl sulfoxide (DMSO; 34.5 mL, 486.7 mmol) in DCM (50 mL) dropwise. The reaction mixture was stirred for 30 min before a solution of the (*R*)-*tert*-butyl 4-(7-hydroxy-5-methyl-6,7-dihydro-5H-cyclopenta[*d*]pyrimidin-4-yl)piperazine-1-carboxylate (58.1 g, 173.8 mmol) in DCM (80 mL) was added slowly. After complete addition, the reaction mixture was stirred for 1 h at –78 °C before triethylamine (TEA; 114 mL, 817.0 mmol) was added slowly. The reaction mixture was then allowed to warm to rt and stirred for 30 min before being quenched with water (200 mL). The organic layer was separated, and the aqueous layer was extracted with DCM (3 × 200 mL). The combined extracts were dried over Na₂SO₄, filtered, and concentrated in vacuo. The residue was purified by silica gel chromatography eluting with DCM–EtOAc (2:1 to 1:3) to give the desired (*R*)-*tert*-butyl 4-(5-methyl-7-oxo-6,7-dihydro-5H-cyclopenta[*d*]pyrimidin-4-yl)piperazine-1-carboxylate (41.0 g, 71% yield) as a brown foam: ¹H NMR (CDCl₃, 400 MHz) δ 8.47 (s, 1H), 3.72–3.68 (m, 2H), 3.57–3.43 (m, 7H), 2.96–2.81 (m, 2H), 2.32–2.26 (m, 1H),

1.73–1.65 (m, 1H), 1.48 (s, 9H), 1.17 (d, *J* = 7.2 Hz, 3H); LC/MS APCI (+) *m/z* 233.1 [M – C₃H₅O₂ + H].

General Procedure for Asymmetric Hydrogenation. *tert*-Butyl 4-((5*R*,7*R*)-7-Hydroxy-5-methyl-6,7-dihydro-5H-cyclopenta[*d*]pyrimidin-4-yl)piperazine-1-carboxylate (**12a**). A round-bottom flask was charged with **10** (17.1 g, 51.4 mmol), DCM (400 mL), formic acid (2.4 mL, 63.3 mmol), and TEA (7.6 mL, 54.5 mmol) and flushed with nitrogen for 15 min. To this solution was added RuCl(*p*-cymene)-[(*R,R*)-TsDPEN] (0.163 g, 0.257 mmol) in one portion, and the reaction mixture was stirred under a nitrogen atmosphere overnight. The reaction mixture was concentrated by rotary evaporation and purified directly by silica gel chromatography eluting with DCM–EtOAc (1:4) to DCM–MeOH (9:1) to give crude *tert*-butyl 4-((5*R*,7*R*)-7-hydroxy-5-methyl-6,7-dihydro-5H-cyclopenta[*d*]pyrimidin-4-yl)piperazine-1-carboxylate (15.2 g, 88.2) as a tan foam. The material was dissolved in DCM (300 mL), cooled to 0 °C under nitrogen, and treated with TEA (18.9 mL, 136.2 mmol) and 4-nitrobenzoyl chloride (12.6 g, 68.1 mmol), respectively. The reaction was stirred, warming to rt for 3 h. The reaction was quenched with saturated aqueous NaHCO₃ and stirred for 5 min before separation of the organic layer. The aqueous layer was extracted with DCM (2 × 200 mL), and the combined organic extracts were washed with brine, dried over Na₂SO₄, and concentrated in vacuo. The crude material was purified by silica gel chromatography eluting with hexanes–EtOAc (5:1) to EtOAc to provide the desired *tert*-butyl 4-((5*R*,7*R*)-5-methyl-7-((4-nitrobenzoyl)oxy)-6,7-dihydro-5H-cyclopenta[*d*]pyrimidin-4-yl)piperazine-1-carboxylate (19.2 g, 87% yield) as a tan foam: ¹H NMR (CDCl₃, 400 MHz) δ 8.60 (s, 1H), 8.28–8.22 (ABq, 4H), 6.35 (t, *J* = 7.2 Hz, 1H), 3.83–3.78 (m, 2H), 3.78–3.49 (m, 7H), 2.40–2.36 (m, 2H), 1.49 (s, 9H), 1.27 (d, *J* = 7.2 Hz, 3H); LC/MS APCI (+) *m/z* 484.1 (M + H)⁺.

tert-Butyl 4-((5*R*,7*R*)-5-methyl-7-((4-nitrobenzoyl)oxy)-6,7-dihydro-5H-cyclopenta[*d*]pyrimidin-4-yl)piperazine-1-carboxylate (19.2 g, 39.7 mmol) was dissolved in THF (150 mL) and water (75 mL). The reaction was cooled to 0 °C and treated with solid LiOH–H₂O (4.2 g, 99.3 mmol). The mixture was stirred for 1 h and concentrated by rotary evaporation. The residue was partitioned between EtOAc (300 mL) and saturated aqueous NaHCO₃ (300 mL). The organic layer was separated, and the aqueous layer was extracted with EtOAc (2 × 150 mL). The combined organic layer was washed with brine, dried over Na₂SO₄, filtered through Celite, and concentrated in vacuo to provide the desired *tert*-butyl 4-((5*R*,7*R*)-7-hydroxy-5-methyl-6,7-dihydro-5H-cyclopenta[*d*]pyrimidin-4-yl)piperazine-1-carboxylate (11.5 g, 87% yield) as a tan powder: ¹H NMR (CDCl₃, 400 MHz) δ 8.57 (s, 1H), 5.12 (t, *J* = 7.2 Hz, 1H), 4.04 (br s, 1H), 3.81–3.75 (m, 2H), 3.67–3.46 (m, 7H), 2.21–2.16 (m, 2H), 1.48 (s, 9H), 1.20 (d, *J* = 7.2 Hz, 3H); LC/MS APCI (+) *m/z* 335.2 (M + H)⁺.

tert-Butyl 4-((5*R*,7*S*)-7-Hydroxy-5-methyl-6,7-dihydro-5H-cyclopenta[*d*]pyrimidin-4-yl)piperazine-1-carboxylate (**13a**). Compound **13a** was prepared from **10** by the same procedure as for compound **12a**, using RuCl(*p*-cymene)-[(*S,S*)-TsDPEN]: ¹H NMR (CDCl₃, 400 MHz) δ 8.56 (s, 1H), 5.04–5.00 (dd, 1H), 3.72–3.67 (m, 2H), 3.63–3.43 (m, 6H), 3.33–3.23 (m, 1H), 2.72 (dt, *J*_d = 13.5 Hz, *J*_t = 8.0 Hz, 1H), 1.66–1.58 (dt, 1H), 1.48 (s, 9H), 1.29 (d, *J* = 6.8 Hz, 3H); LC/MS (APCI) *m/z* 335.2 (M + H)⁺.

General Procedure for Preparation of Fluorinated Cores: *tert*-Butyl 4-((5*R*,7*S*)-7-Fluoro-5-methyl-6,7-dihydro-5H-cyclopenta[*d*]pyrimidin-4-yl)piperazine-1-carboxylate (**14a**). To a solution of **12a** (1.2 g, 3.6 mmol) in DCM (55 mL) at –20 °C was added DAST (1.4 mL, 10.7 mmol). After being stirred for 1 h at –20 °C, the reaction was quenched with ice and warmed to rt. The mixture was diluted with saturated aqueous NH₄Cl, and the layers were separated. The aqueous phase was extracted with DCM (2 × 25 mL), and the combined organic layer was dried over Na₂SO₄, filtered, and concentrated in vacuo. The crude residue was purified by silica gel chromatography eluting with hexanes–EtOAc (2:1) to give the desired *tert*-butyl 4-((5*R*,7*S*)-7-fluoro-5-methyl-6,7-dihydro-5H-cyclopenta[*d*]pyrimidin-4-yl)piperazine-1-carboxylate (0.73 g, 61% yield) as a dark oil: ¹H NMR (CDCl₃, 400 MHz) δ 8.62 (s, 1H), 5.80 (ddd, *J* = 560, 7.2, 3.2 Hz, 1H), 3.78–3.72 (m,

2H), 3.62–3.46 (m, 7H), 2.59–2.46 (m, 1H), 2.08–1.98 (m, 1H), 1.48 (s, 9H), 1.20 (d, $J = 7.2$ Hz, 3H).

General Procedure for Removal of the Boc Group on Piperazine. (5*R*,7*R*)-5-Methyl-4-(piperazin-1-yl)-6,7-dihydro-5*H*-cyclopenta[*d*]pyrimidin-7-ol Dihydrochloride (12*b*). To a solution of 12*a* (11.5 g, 34.4 mmol) in dioxane (100 mL) and DCM (10 mL) was added 4 N HCl in dioxane (117 mL, 471 mmol) by addition funnel at 0 °C. The reaction mixture was warmed to rt and stirred under a nitrogen atmosphere overnight before concentration to dryness by rotary evaporation. The resulting solid was dissolved in a small amount of MeOH (60 mL) and added slowly to a stirring solution of ether (500 mL), resulting in a slurry. The slurry was stirred for 5 min before filtration under a nitrogen atmosphere (hygroscopic). The wet cake was dried under high vacuum to give the desired (5*R*,7*R*)-5-methyl-4-(piperazin-1-yl)-6,7-dihydro-5*H*-cyclopenta[*d*]pyrimidin-7-ol dihydrochloride (9.3 g, 89% yield) as a white solid: ¹H NMR (D₂O, 400 MHz) δ 8.51 (s, 1H), 5.32 (t, $J = 7.2$ Hz, 1H), 4.27–4.23 (m, 2H), 4.09–4.06 (m, 2H), 3.58 (ddd, $J = 7.2$ Hz, 7.2 Hz, 7.2 Hz, 1H), 3.35–3.32 (m, 4H), 2.27–2.22 (m, 1H), 2.11–2.06 (m, 1H), 1.07 (d, $J = 7.2$ Hz, 3H); LC/MS APCI (+) m/z 235.0 (M + H)⁺.

(*R*)-4-Benzyl-3-(2-(4-chlorophenyl)acetyl)oxazolidin-2-one (17). To a stirred solution of (*R*)-4-benzyl-oxazolidin-2-one (16) (48.7 g, 275.0 mmol) in THF (700 mL) at –78 °C was added 2.5 M *n*-BuLi in toluene (107 mL, 267.5 mmol) dropwise by syringe. After complete addition, the reaction was warmed to –20 °C for 1 h. The reaction mixture was cooled again to –78 °C, and 2-(4-chlorophenyl)acetyl chloride (47.2 g, 250 mmol) in THF (50 mL) was added slowly. After complete addition, the mixture was warmed to rt overnight. The reaction was quenched with 1 N HCl, and the partitioned organic layer was separated. The aqueous layer was extracted with EtOAc (2 × 250 mL), and the combined organic layer was dried over MgSO₄, filtered, and concentrated in vacuo. The crude material was purified by column chromatography eluting with hexanes–EtOAc (4:1) to give the desired (*R*)-4-benzyl-3-(2-(4-chlorophenyl)acetyl)oxazolidin-2-one (64.7 g, 79% yield) as a white solid: ¹H NMR (CDCl₃, 400 MHz) δ 7.33–7.26 (m, 7H), 7.13 (d, $J = 6.4$ Hz, 2H), 4.69–4.66 (m, 1H), 4.33–4.16 (m, 4H), 3.60 (dd, $J = 10.2, 3.2$ Hz), 1H), 2.76 (dd, $J = 10.2, 9.6$ Hz, 1H).

General Procedure for the Asymmetric Mannich Reaction. *tert*-Butyl (S)-3-((*R*)-4-Benzyl-2-oxooxazolidin-3-yl)-2-(4-chlorophenyl)-3-oxopropylisopropylcarbamate (19*a*). To a –78 °C solution of (*R*)-4-benzyl-3-(2-(4-chlorophenyl)acetyl)oxazolidin-2-one (10.0 g, 30.3 mmol) in DCM (300 mL) was added 1 M TiCl₄ in toluene (31.8 mL, 31.8 mmol), resulting in an orange solution. Subsequent addition of DIEA (5.8 mL, 33.4 mmol) by syringe gave a dark purple reaction mixture. The reaction was stirred for 15 min before a solution of *tert*-butyl isopropyl(methoxymethyl)carbamate (8.0 g, 39.4 mmol) in DCM (20 mL) was added slowly by syringe. The reaction mixture was stirred for 15 min at –78 °C and then warmed to rt. The reaction was allowed to stir for 1.5 h before being quenched with saturated aqueous NH₄Cl (50 mL). The organic layer was separated, and the aqueous layer was extracted with DCM (2 × 50 mL). The combined organics were washed with brine, dried over Na₂SO₄, and concentrated in vacuo. The crude material was purified by column chromatography eluting with hexanes–EtOAc (5:1) to give the desired *tert*-butyl (S)-3-((*R*)-4-benzyl-2-oxooxazolidin-3-yl)-2-(4-chlorophenyl)-3-oxopropylisopropylcarbamate (10.9 g, 72% yield) as a white foam: ¹H NMR (CDCl₃, 400 MHz) δ 7.35–7.22 (m, 9H), 5.54 (br s, 1H), 4.62–4.58 (m, 1H), 4.13–3.95 (m, 4H), 3.41–3.36 (m, 2H), 2.76 (br s, 1H), 1.48 (s, 9H), 1.08 (d, $J = 6.4$ Hz, 3H), 0.90 (d, $J = 6.4$ Hz, 3H); LC/MS APCI (+) m/z 359.0 [M – C₃H₇O₂ + H].

(S)-3-((*tert*-Butoxycarbonyl)isopropylamino)-2-(4-chlorophenyl)propanoic Acid (20*a*). To a 0 °C solution of LiOH–H₂O (3.1 g, 131.7 mmol) in THF (750 mL) and H₂O (250 mL) was added 35 wt % aqueous hydrogen peroxide (19.2 mL, 197.6 mmol). This solution was stirred for 10 min before a solution of *tert*-butyl (S)-3-((*R*)-4-benzyl-2-oxooxazolidin-3-yl)-2-(4-chlorophenyl)-3-oxopropylisopropylcarbamate (33.0 g, 65.8 mmol) in THF (50 mL) was added. The reaction was warmed to rt overnight. The reaction was quenched by the addition of 10 wt % aqueous Na₂SO₃ (10 mL) and saturated aqueous NaHCO₃ (10 mL). After being stirred for 10 min, the reaction was

concentrated by rotary evaporation to remove THF before extraction of the remaining aqueous layer with ether (3 × 150 mL). The aqueous layer was partitioned with EtOAc (150 mL) and acidified to pH 1 with 1 N HCl. The organic layer was separated, and the aqueous layer was extracted with EtOAc (2 × 150 mL). The combined organic was dried over MgSO₄ and concentrated in vacuo to give the desired (S)-3-((*tert*-butoxycarbonyl)isopropylamino)-2-(4-chlorophenyl)propanoic acid (17.4 g, 77% yield), which was used without further purification: ¹H NMR (CDCl₃, 400 MHz) δ 7.34 (ABq, 4H), 4.16–4.09 (m, 1H), 4.07 (br s, 1H), 3.75 (dd, $J = 14.0, 7.2$ Hz), 1H), 3.30 (dd, $J = 14.0, 7.2$ Hz, 1H), 1.45 (s, 9H), 1.04 (d, $J = 6.8$ Hz, 3H), 0.89 (d, $J = 6.8$ Hz, 3H); LC/MS APCI (+) m/z 242.1 [M – C₅H₉O₂ + H].

***tert*-Butyl (S)-3-((*R*)-4-Benzyl-2-oxooxazolidin-3-yl)-2-(4-chlorophenyl)-3-oxopropyl(2,4-dimethoxybenzyl)carbamate (19*f*).** To a –78 °C solution of (*R*)-4-benzyl-3-(2-(4-chlorophenyl)acetyl)oxazolidin-2-one (6.00 g, 18.2 mmol) in DCM (180 mL) was added 1 M TiCl₄ in toluene (22.7 mL, 22.7 mmol), followed by diisopropylethylamine (3.30 mL, 19.1 mmol), giving rise to a dark purple mixture. The reaction mixture was stirred for 10 min before a solution of *tert*-butyl (2,4-dimethoxybenzyl)(methoxymethyl)carbamate (6.80 g, 21.8 mmol) in DCM (30 mL) was added dropwise. After complete addition, the reaction mixture was stirred for 10 min at –78 °C and then warmed to –10 °C over 3 h. The reaction mixture was quenched with the addition of saturated NH₄Cl solution (50 mL). The resulting mixture was separated, and the aqueous layer was extracted with DCM (3 × 100 mL). The combined organic layers were dried over Na₂SO₄, filtered, and concentrated in vacuo. The crude residue was purified by silica gel chromatography eluting with hexanes–EtOAc (6:1 to 4:1) to provide the pure *tert*-butyl (S)-3-((*R*)-4-benzyl-2-oxooxazolidin-3-yl)-2-(4-chlorophenyl)-3-oxopropyl(2,4-dimethoxybenzyl)carbamate (7.30 g, 66% yield) as a white foam: HPLC (method A) purity 95%; LC/MS APCI (+) m/z 509 (M – Boc + H).

***tert*-Butyl (S)-3-((*R*)-4-Benzyl-2-oxooxazolidin-3-yl)-2-(4-chlorophenyl)-3-oxopropylcarbamate (19*h*).** To a solution of 19*f* (5.30 g, 8.70 mmol) in DCM (80 mL) and H₂O (5 mL) was added 2,3-dichloro-5,6-dicyano-1,4-benzoquinone (DDQ; 2.57 g, 11.3 mmol). The reaction mixture was stirred vigorously at rt for 19 h. The mixture was quenched with saturated NaHCO₃ (10 mL), and the organic layer was washed with saturated NaHCO₃ (2 × 10 mL). The combined aqueous layer was extracted with DCM (2 × 50 mL), and the combined organic layers were dried over Na₂SO₄, filtered, and concentrated in vacuo. The crude was purified by silica gel chromatography eluting with hexanes–EtOAc (9:1 to 5:1) to give the desired *tert*-butyl (S)-3-((*R*)-4-benzyl-2-oxooxazolidin-3-yl)-2-(4-chlorophenyl)-3-oxopropylcarbamate (4.0 g, 100% yield) as a yellow oil: ¹H NMR (CDCl₃, 400 MHz) δ 10.3 (s, 1H), 7.81 (d, $J = 8.6$ Hz, 1H), 7.38–7.19 (m, 6H), 6.58–6.53 (m, 1H), 6.47–6.43 (m, 1H), 5.19–5.11 (m, 1H), 4.84–4.77 (m, 1H), 4.67–4.58 (m, 1H), 4.11–4.03 (m, 1H), 3.76–3.65 (m, 1H), 3.58–3.47 (m, 1H), 3.36–3.26 (m, 1H), 2.90–2.78 (m, 1H), 1.43 (s, 9H); LC/MS APCI (+) m/z 359 (M – Boc + H).

(S)-3-((*tert*-Butoxycarbonyl)amino)-2-(4-chlorophenyl)propanoic Acid (20*h*). To a solution of LiOH–H₂O (0.73 g, 17 mmol) in THF–H₂O (2:1, 83 mL) was added 35 wt % aqueous H₂O₂ (1.8 mL, 22 mmol). The reaction mixture was stirred for 30 min at rt before being cooled to 0 °C. A solution of 19*h* (4.0 g, 8.7 mmol) in THF (40 mL) was added dropwise over a 25 min period, and the reaction mixture was warmed to rt for 12 h. The reaction mixture was cooled to 0 °C again and treated with 1 M Na₂SO₃ (35 mL). The mixture was stirred for 15 min before concentration in vacuo. The mixture was diluted with water (40 mL) and washed twice with ether (2 × 25 mL). The aqueous layer was acidified with solid KHSO₄ and extracted with DCM (2 × 25 mL). The combined organic layers were dried over Na₂SO₄, filtered, and concentrated in vacuo to give the desired (S)-3-((*tert*-butoxycarbonyl)-2-(4-chlorophenyl)propanoic acid (2.8 g, 100% yield) as a crude pale yellow foam. This material was used without further purification: HPLC purity 80%; LC/MS APCI (+) m/z 200 (M – Boc + H).

To a solution of (S)-3-((*tert*-butoxycarbonyl)-2-(4-chlorophenyl)propanoic acid (2.8 g, 9.4 mmol) in dioxane–DCM (2:1, 90 mL) was added slowly 4 N HCl in dioxane (70.8 mL, 283.1 mmol). The reaction mixture was stirred at rt for 17 h before concentration to dryness. The

residue was dissolved in DCM (15 mL) and MeOH (5 mL). The resulting solution was added dropwise to a solution of vigorously stirring ether (300 mL), resulting in a slurry. The slurry was filtered under a nitrogen atmosphere, rinsed with ether (200 mL), and dried in vacuo to give (S)-3-amino-2-(4-chlorophenyl)propanoic acid hydrochloride (1.7 g, 79% yield) as a white solid: $^1\text{H NMR}$ (CD_3OD , 400 MHz) δ 7.42 (d, J = 8.6 Hz, 2H), 7.33 (d, J = 8.6 Hz, 2H), 3.97 (dd, 1H), 3.57–3.54 (m, 1H), 3.24–3.17 (m, 1H); HPLC (method A) purity 97%; LC/MS APCI (+) m/z 200 ($M + \text{H}$).

To a thin slurry of (S)-3-amino-2-(4-chlorophenyl)propanoic acid hydrochloride (1.7 g, 7.4 mmol) and tetramethylammonium hydroxide pentahydrate (3.4 g, 18.5 mmol) in 10:1 MeCN– H_2O (80 mL) was added Boc_2O (3.2 g, 14.8 mmol). The reaction mixture was stirred at rt for 8 h and concentrated by rotary evaporation. The mixture was diluted with 0.5 M NaOH (10 mL) and washed with ether (2×25 mL). The aqueous layer was acidified with solid KHSO_4 and extracted with DCM (2×50 mL). The combined organic layer was dried over Na_2SO_4 , filtered, and concentrated in vacuo. The resulting residue was concentrated from DCM–hexanes mixtures twice to give the desired (S)-3-((*tert*-butoxycarbonyl)amino)-2-(4-chlorophenyl)propanoic acid (2.07 g, 93% yield) as a white foam: $^1\text{H NMR}$ (CDCl_3 , 400 MHz, rotamers present) δ 7.32 (d, J = 8.4 Hz, 2H), 7.22 (d, J = 8.4 Hz, 2H), 3.96–3.85 (m, 0.2H), 3.82–3.73 (m, 0.8 H), 3.67–3.54 (m, 0.4H), 3.54–3.38 (m, 1.6H), 1.48 (s, 5.8H), 1.42 (s, 3.2H); HPLC (method B) purity 97%, >99% ee by chiral HPLC; LC/MS APCI (+) m/z 200 ($M - \text{Boc} + \text{H}$).

General Procedure for Amide Coupling: *tert*-Butyl (S)-2-(4-Chlorophenyl)-3-(4-((5*R*,7*R*)-7-hydroxy-5-methyl-6,7-dihydro-5*H*-cyclopenta[*d*]pyrimidin-4-yl)piperazin-1-yl)-3-oxopropyl-isopropylcarbamate (**24a**). To a solution of **12b** (2.0 g, 6.5 mmol), **20a** (2.2 g, 6.5 mmol), and DIEA (3.6 mL, 20.8 mmol) in DCM (55 mL) at 0 °C was added *N,N,N',N'*-tetramethyl-*O*-(1*H*-benzotriazol-1-yl)-uronium hexafluorophosphate (HBTU; 2.4 g, 6.5 mmol). The reaction mixture was warmed to rt over a 4 h period. The reaction was quenched by the addition of 2 M Na_2CO_3 (5 mL), and the organic layer was separated. The aqueous layer was extracted with DCM (2×25 mL), and the combined organic layer was dried over Na_2SO_4 , filtered, and concentrated in vacuo. The crude material was purified by silica gel chromatography eluting with DCM–EtOAc (1:1 to 1:9) and then DCM–MeOH (30:1). The crude product was dissolved in DCM (10 mL) and hexanes (100 mL). The resulting slurry was cooled to 0 °C and filtered to give the desired *tert*-butyl (S)-2-(4-chlorophenyl)-3-(4-((5*R*,7*R*)-7-hydroxy-5-methyl-6,7-dihydro-5*H*-cyclopenta[*d*]pyrimidin-4-yl)piperazin-1-yl)-3-oxopropyl)isopropylcarbamate (3.2 g, 87% yield) as a white powder: $^1\text{H NMR}$ (CDCl_3 , 400 MHz) δ 8.49 (s, 1H), 7.34 (d, J = 8.4 Hz, 2H), 7.29 (d, J = 8.4 Hz, 2H), 5.09 (t, J = 7.2 Hz, 1H), 3.78–3.31 (m, 15H), 2.18–2.14 (m, 2H), 1.47 (s, 9H), 1.13 (d, J = 7.2 Hz, 3H), 0.97–0.95 (m, 3H), 0.68–0.67 (m, 2H); LC/MS APCI (+) m/z 458.2 [$M - \text{C}_5\text{H}_9\text{O}_2 + \text{H}$].

General Procedure for Boc Deprotection. (S)-2-(4-Chlorophenyl)-1-(4-((5*R*,7*R*)-7-hydroxy-5-methyl-6,7-dihydro-5*H*-cyclopenta[*d*]pyrimidin-4-yl)piperazin-1-yl)-3-(isopropylamino)propan-1-one Dihydrochloride Salt (**28**). To a solution of **24a** (2.5 g, 4.5 mmol) in dioxane (25 mL) was added 4 M HCl in dioxane (22.4 mL, 89.6 mmol). The resulting solution was stirred overnight at rt before concentration by rotary evaporation to a gel. This gel was dissolved in a small amount of MeOH (10 mL) followed by addition to ether (300 mL) to give a white slurry. The resulting slurry was filtered under a nitrogen atmosphere and subsequently dried under a nitrogen flow to give the desired (S)-2-(4-chlorophenyl)-1-(4-((5*R*,7*R*)-7-hydroxy-5-methyl-6,7-dihydro-5*H*-cyclopenta[*d*]pyrimidin-4-yl)piperazin-1-yl)-3-(isopropylamino)propan-1-one dihydrochloride salt (2.1 g, 90% yield) as a light yellow solid: $^1\text{H NMR}$ (CD_3OD , 400 MHz) δ 8.58 (s, 1H), 7.45 (d, J = 8.4 Hz, 2H), 7.40 (d, J = 8.4 Hz, 2H), 5.31 (appt, J = 8.0 Hz, 1H), 4.58 (dd, J = 9.6, 4.0 Hz, 1H), 4.19 (m, 1H), 4.05–3.89 (m, 3H), 3.82–3.65 (m, 5H), 3.48–3.41 (m, 2H), 3.17 (dd, J = 12.4, 3.6 Hz, 1H), 2.30 (dd, J = 12.8, 7.6 Hz, 1H), 2.19 (ddd, J = 16.4, 12.8, 8.0 Hz, 1H), 1.37 (d, J = 6.4 Hz, 6H), 1.19 (d, J = 6.8 Hz, 3H); LC/MS APCI (+) m/z 458 ($M + \text{H}$)⁺; HPLC (method B) >99% purity, t_R = 1.83 min.

(S)-2-(4-Chlorophenyl)-3-(isopropylamino)-1-(4-((*R*)-5-methyl-6,7-dihydro-5*H*-cyclopenta[*d*]pyrimidin-4-yl)piperazin-1-yl)propan-1-one Dihydrochloride Salt (**3**). Compound **3** was prepared from **8a** and **20a** by the same procedure as described for **28**: $^1\text{H NMR}$ (D_2O , 400 MHz) δ 8.30 (s, 1H), 7.36 (d, J = 8.6 Hz, 2H), 7.22 (d, J = 8.6 Hz, 2H), 4.31 (dd, J = 8.2, 4.7 Hz, 1H), 4.16–4.04 (m, 1H), 3.92–3.82 (m, 1H), 3.80–3.70 (m, 1H), 3.70–3.58 (m, 1H), 3.58–3.40 (m, 6H), 3.35 (d, J = 6.5 Hz, 1H), 3.21 (dd, J = 12.9, 4.7 Hz, 1H), 2.97 (d, J = 9.0 Hz, 1H), 2.82 (ddd, J = 18.3, 9.8, 2.7 Hz, 1H), 2.30–2.16 (m, 1H), 1.78–1.68 (m, 1H), 1.20 (d, J = 4.4 Hz, 3H), 1.19 (d, J = 4.0 Hz, 3H), 0.94 (d, J = 6.6 Hz, 3H); LC/MS APCI (+) m/z 442 ($M + \text{H}$)⁺; HPLC (method A) >99% purity, t_R = 1.86 min.

(S)-2-(4-Chlorophenyl)-1-(4-(5,5-dimethyl-6,7-dihydro-5*H*-cyclopenta[*d*]pyrimidin-4-yl)piperazin-1-yl)-3-(isopropylamino)propan-1-one Bis(trifluoroacetate) Salt (**25**). Compound **25** was prepared from **8b** and **20a** by the same procedure described for **28**: $^1\text{H NMR}$ ($\text{DMSO-}d_6$, 400 MHz) δ 8.45 (s, 1H), 7.36 (dd, J = 20.9, 8.5 Hz, 4H), 4.17 (dd, J = 8.2, 5.6 Hz, 1H), 3.74–3.55 (m, 3H), 3.51–3.38 (m, 1H), 3.27–3.04 (m, 4H), 2.95–2.57 (m, 6H), 1.81 (t, J = 7.2 Hz, 2H), 1.32 (d, J = 4.9 Hz, 6H), 0.93 (dd, J = 7.4, 6.4 Hz, 6H); LC/MS m/z 456 ($M + \text{H}$)⁺; HPLC (method E) 97.9% purity, t_R = 3.38 min.

(S)-2-(4-Chlorophenyl)-3-(isopropylamino)-1-(4-((*S*)-5-vinyl-6,7-dihydro-5*H*-cyclopenta[*d*]pyrimidin-4-yl)piperazin-1-yl)propan-1-one (**26**). Compound **26** was prepared from **8c** and **20a** by the same procedure described for **28**: $^1\text{H NMR}$ ($\text{DMSO-}d_6$, 400 MHz) δ 8.35 (s, 1H), 7.36 (dd, J = 8.0, 8.5 Hz, 4H), 5.85 (ddd, J = 17.2, 10.2, 7.0 Hz, 1H), 4.99 (d, J = 10.2 Hz, 1H), 4.81 (d, J = 17.2 Hz, 1H), 4.18 (dd, J = 8.4, 5.6 Hz, 1H), 4.04 (m, 1H), 3.45–3.70 (m, 7H), 3.13 (dd, J = 11.6, 8.6 Hz, 2H), 3.06 (d, J = 10.0 Hz, 1H), 2.80–2.61 (m, 4H), 2.21 (m, 1H), 1.74 (m, 1H), 0.95 (t, J = 6.6 Hz, 6H); LC/MS APCI (+) m/z 454.2 ($M + 1$); HPLC (method D) 98% purity, t_R = 3.88 min.

(S)-2-(4-Chlorophenyl)-1-(4-((*R*)-5-(hydroxymethyl)-6,7-dihydro-5*H*-cyclopenta[*d*]pyrimidin-4-yl)piperazin-1-yl)-3-(isopropylamino)propan-1-one (**27**). Compound **27** was prepared from **8d** and **20a** by the same procedure described for **28**: $^1\text{H NMR}$ (CD_3OD , 500 MHz) δ 8.39 (s, 1H), 7.40 (d, J = 8.4 Hz, 2H), 7.23 (d, J = 8.4 Hz, 2H), 4.18 (m, 1H), 4.08 (m, 1H), 3.90 (m, 1H), 3.75 (m, 1H), 3.69–3.48 (m, 7H), 3.42 (m, 3H), 3.27 (m, 1H), 3.07–2.82 (m, 2H), 2.25 (m, 1H), 2.04 (m, 1H), 1.25 (t, J = 6.6 Hz, 6H); LC/MS APCI (+) m/z 458.2 ($M + 1$); HPLC (method E) 100% purity, t_R = 6.47 min.

(S)-2-(4-Chlorophenyl)-1-(4-((5*R*,7*S*)-7-hydroxy-5-methyl-6,7-dihydro-5*H*-cyclopenta[*d*]pyrimidin-4-yl)piperazin-1-yl)-3-(isopropylamino)propan-1-one Dihydrochloride Salt (**29**). Compound **29** was prepared from **13b** and **20a** by the same procedure described for **28**: $^1\text{H NMR}$ (D_2O , 400 MHz) δ 8.39 (s, 1H), 7.36 (d, J = 8.4 Hz, 2H), 7.21 (d, J = 8.4 Hz, 2H), 5.08 (dd, J = 8.4, 4.8 Hz, 1H), 4.30 (dd, J = 8.0, 4.8 Hz, 1H), 4.15 (m, 1H), 3.84 (m, 1H), 3.69 (m, 1H), 3.56–3.43 (m, 5H), 3.41–3.32 (m, 2H), 3.22 (dd, J = 12.8, 4.8 Hz, 1H), 2.67 (ddd, J = 14.4, 8.0, 4.0 Hz, 1H), 1.51 (ddd, J = 14.0, 10.0, 4.0 Hz, 1H), 1.38 (d, J = 7.2 Hz, 1H), 1.19 (dd, J = 6.4, 4.4 Hz, 6H), 1.04 (d, J = 7.2 Hz, 3H); LC/MS APCI (+) m/z 458 ($M + \text{H}$)⁺; HPLC (method A) >95% purity, t_R = 1.82 min.

(S)-2-(4-Chlorophenyl)-1-(4-((5*R*,7*R*)-7-fluoro-5-methyl-6,7-dihydro-5*H*-cyclopenta[*d*]pyrimidin-4-yl)piperazin-1-yl)-3-(isopropylamino)propan-1-one Bis(trifluoroacetate) Salt (**30**). Compound **30** was prepared from **15b** and **20a** by the same procedure described for **28**: $^1\text{H NMR}$ (D_2O , 400 MHz) δ 8.52 (s, 1H), 7.50 (d, J = 8.0 Hz, 2H), 7.37 (d, J = 8.0 Hz, 2H), 5.71 (td, J = 56.0, 8.0 Hz, 1H), 4.42 (m, 2H), 3.93–3.83 (m, 1H), 3.78–3.68 (m, 1H), 3.60–3.30 (m, 7H), 3.20–3.00 (m, 2H), 2.65–2.50 (m, 1H), 1.77 (dd, J = 28, 8 Hz, 1H), 1.23 (m, 6H), 1.14 (d, J = 8.0 Hz, 3H); LC/MS APCI (+) m/z 460 ($M + \text{H}$)⁺; HPLC (method C) 99% purity, t_R = 3.84 min.

(S)-2-(4-Chlorophenyl)-1-(4-((5*R*,7*S*)-7-fluoro-5-methyl-6,7-dihydro-5*H*-cyclopenta[*d*]pyrimidin-4-yl)piperazin-1-yl)-3-(isopropylamino)propan-1-one Bis(trifluoroacetate) Salt (**31**). Compound **31** was prepared from **14b** and **20a** by the same procedure described for **28**: $^1\text{H NMR}$ (D_2O , 400 MHz) δ 8.54 (s, 1H), 7.50 (d, J = 8.0 Hz, 2H), 7.37 (d, J = 8.0 Hz, 2H), 5.86 (dt, J = 56.0, 4.0 Hz, 1H), 4.47 (m, 2H), 3.90–3.78 (m, 3H), 3.83 (m, 1H), 3.70 (m, 1H), 3.62–3.50 (m, 5H), 3.18–3.00 (m, 2H), 2.45–2.30 (m, 1H), 2.12–1.98 (m, 1H),

1.23 (m, 6H), 1.06 (d, $J = 8.0$ Hz, 3H); LC/MS APCI (+) m/z 460 (M + H)⁺; HPLC (method C) >99% purity, $t_R = 3.92$ min.

(*S*)-2-(4-Chlorophenyl)-1-(4-((*R*)-7,7-difluoro-5-methyl-6,7-dihydro-5H-cyclopenta[d]pyrimidin-4-yl)piperazin-1-yl)-3-(isopropylamino)propan-1-one Dihydrochloride Salt (**32**). Compound **32** was prepared from **11b** and **20a** by the same procedure described for **28**: ¹H NMR (D₂O, 400 MHz) δ 8.28 (s, 1H), 7.32 (d, $J = 8.6$ Hz, 2H), 7.18 (d, $J = 8.6$ Hz, 2H), 4.28 (dd, $J = 8.4, 4.9$ Hz, 1H), 3.94–3.80 (m, 2H), 3.58–3.38 (m, 7H), 3.33 (d, $J = 6.6$ Hz, 1H), 3.19 (dd, $J = 12.8, 4.8$ Hz, 1H), 3.12–3.02 (m, 1H), 2.76–2.56 (m, 1H), 2.20–2.04 (m, 1H), 1.19 (d, $J = 4.0$ Hz, 3H), 1.17 (d, $J = 4.0$ Hz, 3H), 0.98 (d, $J = 7.0$ Hz, 3H); LC/MS APCI (+) m/z 478 (M + H)⁺; HPLC (method B) >99% purity, $t_R = 2.27$ min.

(*S*)-2-(4-Chlorophenyl)-1-(4-((*R*)-5-(fluoromethyl)-6,7-dihydro-5H-cyclopenta[d]pyrimidin-4-yl)piperazin-1-yl)-3-(isopropylamino)propan-1-one (**33**). Compound **33** was prepared from **8e** and **20a** by the same procedure described for **28**: ¹H NMR (CD₃OD, 400 MHz) δ 8.59 (s, 1H), 7.41 (m, 4H), 4.20 (m, 1H), 4.07 (m, 1H), 3.98–3.84 (m, 3H), 3.62–3.80 (m, 5H), 3.60–3.40 (m, 4H), 3.27–2.92 (m, 4H), 2.40 (m, 1H), 2.15 (m, 1H), 1.37 (m, 6H); LC/MS APCI (+) m/z 460.2 (M + 1); HPLC (method C) 88% purity, $t_R = 3.48$ min.

(*S*)-3-Amino-2-(4-chlorophenyl)-1-(4-((*S*,*R*)-7-hydroxy-5-methyl-6,7-dihydro-5H-cyclopenta[d]pyrimidin-4-yl)piperazin-1-yl)propan-1-one Dihydrochloride Salt (**34**). Compound **34** was prepared from **12b** and **20f** by the same procedure described for **28**: ¹H NMR (D₂O, 400 MHz) δ 8.39 (s, 1H), 7.37 (d, $J = 8.4$ Hz, 2H), 7.22 (d, $J = 8.4$ Hz, 2H), 5.27 (appt, $J = 7.6$ Hz, 1H), 4.30 (dd, $J = 6.4$ Hz, 1H), 4.11 (m, 1H), 3.88–3.80 (m, 2H), 3.70 (dd, $J = 6.4, 4.4$ Hz, 1H), 3.69–3.65 (m, 1H), 3.63–3.60 (m, 2H), 3.56–3.53 (m, 2H), 3.26 (dd, $J = 13.2, 5.6$ Hz, 1H), 2.20 (dd, $J = 13.2, 8.0$ Hz, 1H), 2.03 (ddd, $J = 16.0, 12.8, 8.0$ Hz, 1H), 1.21 (d, $J = 6.4$ Hz, 1H), 0.97 (d, $J = 6.4$ Hz, 3H); LC/MS APCI (+) m/z 416 (M + H)⁺; HPLC (method B) 98.5% purity, $t_R = 1.72$ min.

(*S*)-2-(4-Chlorophenyl)-3-((cyclopropylmethyl)amino)-1-(4-((*S*,*R*)-7-hydroxy-5-methyl-6,7-dihydro-5H-cyclopenta[d]pyrimidin-4-yl)piperazin-1-yl)propan-1-one Dihydrochloride Salt (**35**). Compound **35** was prepared from **12b** and **20b** by the same procedure described for **28**: ¹H NMR (D₂O, 400 MHz) δ 0.38 (2H, d, $J = 5.3$ Hz), 0.71 (2H, d, $J = 7.2$ Hz), 1.18 (3H, t, $J = 6.9$ Hz), 2.19 (1H, dd, $J = 8.0, 14.6$ Hz), 2.36 (1H, dd, $J = 7.7, 13.0$ Hz), 3.01 (2H, d, $J = 7.2$ Hz), 3.30 (1H, m), 3.49 (1H, dd, $J = 5.1, 12.9$ Hz), 3.57–3.75 (m, 8H), 3.92 (1H, m), 4.07–4.19 (3H, m), 4.52 (1H, dd, $J = 5.5, 7.8$ Hz), 5.43 (1H, t, $J = 7.9$ Hz), 7.39 (2H, d, $J = 8.4$ Hz), 7.53 (2H, d, $J = 8.4$ Hz), 8.55 (1H, s); LC/MS APCI (+) m/z 470 [M + H]⁺; HPLC (method B), 97% purity, $t_R = 1.86$ min.

(*S*)-2-(4-Chlorophenyl)-3-((2-fluoroethyl)amino)-1-(4-((*S*,*R*)-7-hydroxy-5-methyl-6,7-dihydro-5H-cyclopenta[d]pyrimidin-4-yl)piperazin-1-yl)propan-1-one (**36**). Compound **36** was prepared from **12b** and **20c** by the same procedure described for **28**: ¹H NMR (CD₃OD, 400 MHz) δ 8.58 (s, 1H), 7.46 (d, $J = 8.4$ Hz, 2H), 7.39 (d, $J = 8.4$ Hz, 2H), 5.31 (t, $J = 8.0$ Hz, 1H), 4.72 (t, $J = 4.4$ Hz, 1H), 4.61 (dd, $J = 8.4, 4.4$ Hz, 1H), 4.01–3.66 (m, 8H), 3.51–3.41 (m, 4H), 2.32–2.27 (m, 1H), 2.22–2.17 (m, 1H), 1.39–1.35 (m, 3H), 1.18 (d, $J = 6.8$ Hz, 3H); LC/MS APCI (+) m/z 462.2 (M + H)⁺; HPLC (method B) 99% purity, $t_R = 2.24$ min.

(*S*)-2-(4-Chlorophenyl)-1-(4-((*S*,*R*)-7-hydroxy-5-methyl-6,7-dihydro-5H-cyclopenta[d]pyrimidin-4-yl)piperazin-1-yl)-3-((2-methoxyethyl)amino)propan-1-one Dihydrochloride Salt (**38**). Compound **38** was prepared from **12b** and **20d** by the same procedure described for **28**: ¹H NMR (CD₃OD, 400 MHz) δ 8.58 (s, 1H), 7.46 (d, $J = 8.4$ Hz, 2H), 7.38 (d, $J = 8.4$ Hz, 2H), 5.32 (appt, $J = 8.0$ Hz, 1H), 4.56 (dd, $J = 9.6, 4.0$ Hz, 1H), 4.25–4.18 (m, 1H), 4.01–3.91 (m, 2H), 3.84–3.82 (m, 1H), 3.75–3.65 (m, 8H), 3.48 (q, $J = 6.8$ Hz, 2H), 3.41 (s, 3H), 3.31–3.26 (m, 2H), 2.30 (dd, $J = 13.2, 7.6$ Hz, 1H), 2.19 (ddd, $J = 13.2, 8.4, 3.6$ Hz, 1H), 1.18 (d, $J = 6.8$ Hz, 3H); LC/MS APCI (+) m/z 474.1 (M + H)⁺; HPLC (method B) >99% purity, $t_R = 1.81$ min.

(*S*)-2-(3-Fluoro-4-(trifluoromethyl)phenyl)-3-((1-hydroxy-2-methylprop-2-yl)amino)-1-(4-((*S*,*R*)-7-hydroxy-5-methyl-6,7-dihydro-5H-cyclopenta[d]pyrimidin-4-yl)piperazin-1-yl)propan-1-one Bis-(trifluoroacetate) Salt (**39**). Compound **39** was prepared from **12b** and **20e** by the same procedure described for **28**: ¹H NMR (D₂O, 400 MHz) δ 8.58 (s, 1H), 7.86 (dd, $J = 8.0, 5.6$ Hz, 1H), 7.49 (d, $J = 8.0$ Hz,

1H), 7.36 (d, $J = 5.6$ Hz, 1H), 5.07 (m, 1H), 4.50 (m, 1H), 3.91 (m, 2H), 3.80–3.60 (m, 4H), 3.40–3.22 (m, 5H), 3.04 (m, 2H), 2.02 (m, 2H), 1.22 (m, 6H), 1.04 (d, $J = 8.0$ Hz, 6H); LC/MS APCI (+) m/z 540 (M + H)⁺; HPLC (method C) 98.3% purity, $t_R = 3.90$ min.

(*S*)-2-(4-Chlorophenyl)-3-(cyclohexylamino)-1-(4-((*S*,*R*)-7-hydroxy-5-methyl-6,7-dihydro-5H-cyclopenta[d]pyrimidin-4-yl)piperazin-1-yl)propan-1-one Dihydrochloride Salt (**41**). Compound **41** was prepared from **12b** and **20e** by the same procedure described for **28**: ¹H NMR (D₂O, 400 MHz) δ 8.37 (s, 1H), 7.28 (ABq, 4H), 5.29 (t, $J = 7.2$ Hz, 1H), 4.32–4.27 (m, 1H), 4.18–4.10 (m, 1H), 3.88–3.78 (m, 2H), 3.71–3.62 (m, 1H), 3.56–3.44 (m, 5H), 3.28–3.20 (m, 2H), 3.04–2.98 (m, 1H), 2.21–2.16 (m, 1H), 2.05–1.99 (m, 1H), 1.94–1.88 (m, 2H), 1.70–1.68 (m, 2H), 1.53–1.50 (m, 1H), 1.24–1.56 (m, 4H), 1.06–1.03 (m, 1H), 0.96 (d, $J = 7.2$ Hz, 3H); LC/MS APCI (+) m/z 498.3 (M + H)⁺; HPLC (method B) >99% purity, $t_R = 2.01$ min.

(*S*)-2-(4-Chlorophenyl)-1-(4-((*S*,*R*)-7-hydroxy-5-methyl-6,7-dihydro-5H-cyclopenta[d]pyrimidin-4-yl)piperazin-1-yl)-3-(isopropylmethylamino)propan-1-one Dihydrochloride Salt (**42**). A solution of **28** (0.040 g, 0.075 mmol), DIEA (0.039 mL, 0.23 mmol), and 37% formaldehyde (0.056 mL, 0.75 mmol) in 1:1 DCE–THF (0.8 mL) was stirred for 10 min. NaBH(OAc)₃ (0.024 g, 0.11 mmol) was added. The reaction mixture was stirred at rt for 6 h. Saturated NaHCO₃ was added, and the mixture was extracted with DCM. The combined extracts were dried (Na₂SO₄), filtered, and concentrated. The crude was purified by flash column chromatography with silica gel (6:1 DCM–MeOH) to give the free base, which was converted to (*S*)-2-(4-chlorophenyl)-1-(4-((*S*,*R*)-7-hydroxy-5-methyl-6,7-dihydro-5H-cyclopenta[d]pyrimidin-4-yl)piperazin-1-yl)-3-(isopropylmethylamino)propan-1-one dihydrochloride (0.031 g, 76% yield) by treatment with 2 M HCl in diethyl ether: ¹H NMR (D₂O, 400 MHz, note that rotamers were observed) δ 8.37 (s, 1H), 7.38 (d, $J = 8.6$ Hz, 0.4H), 7.35 (d, $J = 8.6$ Hz, 1.6H), 7.27 (d, $J = 8.6$ Hz, 0.4H), 7.21 (d, $J = 8.6$ Hz, 1.6H), 5.26 (t, $J = 8.0$ Hz, 1H), 4.47 (dd, $J = 11.0, 3.5$ Hz, 1H), 4.18–4.06 (m, 1H), 3.92–3.42 (m, 9H), 3.34–3.20 (m, 1H), 3.00 (dd, $J = 12.9, 3.5$ Hz, 1H), 2.74 (s, 2.3H), 2.68 (s, 0.7H), 2.19 (dd, $J = 13.1, 7.6$ Hz, 1H), 2.08–1.98 (m, 1H), 1.26 (d, $J = 6.7$ Hz, 2.3H), 1.20 (d, $J = 6.7$ Hz, 0.7H), 1.18 (d, $J = 6.7$ Hz, 2.3H), 1.15 (d, $J = 6.7$ Hz, 0.7H), 0.97 (d, $J = 7.0$ Hz, 3H); LC/MS APCI (+) m/z 472 (M + H)⁺; HPLC (method B) 99% purity, $t_R = 1.89$ min.

(*S*)-2-(4-Chlorophenyl)-1-(4-((*S*,*R*)-7-hydroxy-5-methyl-6,7-dihydro-5H-cyclopenta[d]pyrimidin-4-yl)piperazin-1-yl)-2-((*S*)-pyrrolidin-2-yl)ethanone Dihydrochloride Salt (**43**). Compound **43** was prepared from **12b** and **23i** by the same procedure described for **28**: ¹H NMR (CD₃OD, 400 MHz) δ 8.57 (s, 1H), 7.45 (d, $J = 8.6, 2H$), 7.41 (d, $J = 8.6, 2H$), 5.31 (t, $J = 8.0, 1H$), 4.51–4.45 (m, 1H), 4.23–3.28 (mm, 11H), 2.33–2.26 (m, 1H), 2.23–2.16 (m, 1H), 2.16–2.06 (m, 1H), 1.98–1.84 (m, 1H), 1.84–1.72 (m, 1H), 1.40–1.34 (m, 2H), 1.18 (d, $J = 7.0, 3H$); LC/MS APCI (+) m/z 456.1, 458.1 (M + H)⁺; HPLC (method A) >97% purity, $t_R = 2.56$ min.

General Procedure for Reductive Amination. (*S*)-2-(4-Chlorophenyl)-1-(4-((*S*,*R*)-7-hydroxy-5-methyl-6,7-dihydro-5H-cyclopenta[d]pyrimidin-4-yl)piperazin-1-yl)-3-((tetrahydro-2H-pyran-4-yl)amino)propan-1-one Dihydrochloride Salt (**44**). A solution of **34** (0.075 g, 0.15 mmol) in 2 M Na₂CO₃ (20 mL) was saturated with NaCl and extracted three times with DCM. The combined extracts were dried (Na₂SO₄), filtered, and concentrated. The resulting residue was dissolved in DCE (2.5 mL). Tetrahydropyran-4-one (0.021 mL, 0.23 mmol) was added, and the solution was stirred at rt for 5 min. NaBH(OAc)₃ (0.065 g, 0.31 mmol) was then added, and the reaction mixture was stirred at rt for 13 h. Saturated NaHCO₃ was added, and the mixture was extracted with DCM. The combined extracts were dried (Na₂SO₄), filtered, and concentrated. The crude material was purified by flash column chromatography with silica gel (6:1 DCM–MeOH) to give the free base, which was converted to (*S*)-2-(4-chlorophenyl)-1-(4-((*S*,*R*)-7-hydroxy-5-methyl-6,7-dihydro-5H-cyclopenta[d]pyrimidin-4-yl)piperazin-1-yl)-3-((tetrahydro-2H-pyran-4-yl)amino)propan-1-one dihydrochloride (0.041 g, 47% yield) by treatment with 2 M HCl in diethyl ether: ¹H NMR (D₂O, 400 MHz) δ 8.36 (s, 1H), 7.35 (d, $J = 8.6$ Hz, 2H), 7.21 (d, $J = 8.6$ Hz, 2H), 5.24 (t, $J = 7.8$ Hz, 1H), 4.31 (dd, $J = 8.4, 4.9$ Hz, 1H), 4.14–4.04 (m, 1H), 3.93 (d, $J = 11.7$ Hz, 2H), 3.90–3.82 (m, 1H), 3.82–3.72 (m, 1H), 3.70–3.60 (m, 1H), 3.60–3.40

(m, 5H), 3.40–3.30 (m, 3H), 3.30–3.20 (m, 2H), 2.18 (dd, $J = 13.3$, 7.4 Hz, 1H), 2.08–1.99 (m, 1H), 1.99–1.87 (m, 2H), 1.59 (dd, $J = 12.1$, 4.7 Hz, 2H), 0.96 (d, $J = 7.0$ Hz, 3H); LC/MS APCI (+) m/z 500 (M + H)⁺; HPLC (method B) 99% purity, $t_R = 1.86$ min.

(*S*)-2-(4-Chlorophenyl)-1-(4-((5*R*,7*R*)-7-hydroxy-5-methyl-6,7-dihydro-5*H*-cyclopenta[*d*]pyrimidin-4-yl)piperazin-1-yl)-3-(((1*R*,4*S*)-4-methoxycyclohexyl)amino)propan-1-one (45). Compound 45 was prepared from 12b and 20g by the same procedure described for 28: ¹H NMR (CDCl₃, 400 MHz) δ 11.11 (br s, 1H), 8.45 (s, 1H), 7.20 (ABq, 4H), 6.62 (br s, 1H), 5.44–5.42 (m, 1H), 4.78–4.67 (m, 1H), 4.14–3.48 (m, 9H), 3.34 (s, 3H), 3.21–3.06 (m, 4H), 2.27–2.18 (m, 6H), 1.60–1.56 (m, 2H), 1.34–1.28 (m, 2H), 1.16 (t, $J = 6.0$ Hz, 3H); LC/MS APCI (+) m/z 528 (M + H)⁺; HPLC (method B) 98% purity, $t_R = 1.95$ min.

(*S*)-2-(4-Chlorophenyl)-1-(4-((5*R*,7*R*)-7-hydroxy-5-methyl-6,7-dihydro-5*H*-cyclopenta[*d*]pyrimidin-4-yl)piperazin-1-yl)-3-(((tetrahydro-2*H*-pyran-4-yl)methyl)amino)propan-1-one (46). Compound 46 was prepared from 34 and tetrahydro-2*H*-pyran-4-carbaldehyde by the same procedure described for 44: ¹H NMR (D₂O, 400 MHz) δ 8.34 (s, 1H), 7.28 (ABq, 4H), 5.21 (t, $J = 7.2$ Hz, 1H), 4.30 (dd, $J = 5.2$, 5.2 Hz, 1H), 4.11–4.05 (m, 1H), 3.87–3.83 (m, 3H), 3.76–3.73 (m, 1H), 3.66–3.62 (m, 1H), 3.52–3.42 (m, 5H), 3.37–3.24 (m, 4H), 2.93–2.82 (m, 2H), 2.19–2.13 (m, 1H), 2.05–1.92 (m, 2H), 1.58–1.55 (m, 2H), 1.27–1.16 (m, 2H), 0.95 (d, $J = 7.2$ Hz, 3H); LC/MS APCI (+) m/z 514.3 (M + H)⁺; HPLC (method B) >99% purity, $t_R = 1.88$ min.

(*S*)-2-(4-Chlorophenyl)-1-(4-((5*R*,7*R*)-7-hydroxy-5-methyl-6,7-dihydro-5*H*-cyclopenta[*d*]pyrimidin-4-yl)piperazin-1-yl)-2-((*S*)-piperidin-2-yl)ethanone Dihydrochloride Salt (47). Compound 47 was prepared from 12b and 23j by the same procedure described for 28: ¹H NMR (D₂O, 400 MHz) δ 8.36 (s, 1H), 7.35 (d, $J = 8.6$ Hz, 2H), 7.20 (d, $J = 8.6$ Hz, 2H), 5.26 (t, $J = 7.8$ Hz, 1H), 4.16–4.06 (m, 2H), 3.92–3.84 (m, 1H), 3.84–3.75 (m, 1H), 3.70–3.61 (m, 1H), 3.61–3.45 (m, 4H), 3.36–3.18 (m, 2H), 2.87 (t, $J = 13.1$ Hz, 1H), 2.19 (dd, $J = 13.3$, 7.8 Hz, 1H), 2.08–1.97 (m, 1H), 1.73 (app. t, $J = 16.8$ Hz, 2H), 1.54 (app. t, $J = 16.4$ Hz, 2H), 1.48–1.25 (m, 3H), 0.96 (d, $J = 6.6$ Hz, 3H); LC/MS APCI (+) m/z 470 (M + H)⁺; HPLC (method B) 99% purity, $t_R = 1.87$ min.

(*S*)-2-(4-Chlorophenyl)-1-(4-((5*R*,7*R*)-7-hydroxy-5-methyl-6,7-dihydro-5*H*-cyclopenta[*d*]pyrimidin-4-yl)piperazin-1-yl)-2-((*R*)-morpholin-3-yl)ethanone Hydrochloride Salt (48). Compound 48 was prepared from 12b and 23k by the same procedure described for 28: ¹H NMR (CD₃OD, 400 MHz) δ 8.57 (s, 1H), 7.48 (d, $J = 8.6$ Hz, 2H), 7.40 (d, $J = 8.6$ Hz, 2H), 5.28 (t, $J = 7.8$, 1H), 4.51 (d, $J = 9.0$ Hz, 1H), 4.17–4.10 (m, 1H), 4.02–3.19 (m, 15H), 2.32–2.24 (m, 1H), 2.22–2.13 (m, 1H), 1.17 (d, $J = 7.0$ Hz, 3H); LC/MS APCI (+) m/z 472.1, 474.1 (M + H)⁺; HPLC (method A) >95% purity, $t_R = 2.40$ min.

Potassium 2-(4-Chlorophenyl)-3-((2,2,2-trifluoroethyl)amino)propanoate (58a). A solution of methyl 3-amino-2-(4-chlorophenyl)propanoate hydrochloride (215 mg, 0.860 mmol) in 1:1 THF–DMF (3.0 mL) was treated with DIEA (389 μ L, 2.23 mmol) at rt. Trifluoroethyl triflate (299 mg, 1.29 mmol) was added to the mixture, and the reaction mixture was stirred for 20 h. The mixture was partitioned between ethyl acetate and diluted NaHCO₃ solution. The aqueous portion was extracted twice, and the combined organics were washed with water (3 \times). The organic portion was washed with brine, separated, dried over MgSO₄, filtered, and concentrated in vacuo. The residue was purified by silica gel column chromatography (4:1 hexanes–EtOAc) to afford methyl 2-(4-chlorophenyl)-3-((2,2,2-trifluoroethyl)amino)propanoate (235 mg, 93% yield) as a colorless oil: ¹H NMR (CDCl₃, 400 MHz) δ 7.33–7.29 (m, 2H), 7.24–7.20 (m, 2H), 3.76–3.71 (dd, 1H), 3.69 (s, 3H), 3.38–3.30 (m, 1H), 3.24–3.12 (m, 2H), 3.05–2.97 (m, 1H); LC/MS APCI (+) m/z 296 (M + H)⁺.

A solution of methyl 2-(4-chlorophenyl)-3-((2,2,2-trifluoroethyl)amino)propanoate (235 mg, 0.795 mmol) in THF (3.0 mL) was treated with KO(TMS) (153 mg, 1.19 mmol) at rt. The reaction mixture was stirred for 18 h before the mixture was diluted with diethyl ether. The resulting precipitate was isolated by filtration and dried in vacuo to give potassium 2-(4-chlorophenyl)-3-((2,2,2-trifluoroethyl)amino)propanoate (299 mg, 100% yield) as a white solid: ¹H NMR (CD₃OD, 400 MHz) δ 7.33 (d, $J = 8.4$ Hz, 2H), 7.25 (d, $J = 8.4$ Hz,

2H), 3.65–3.60 (m, 1H), 3.27–3.18 (m, 3H), 2.86–2.80 (m, 1H); LC/MS APCI (+) m/z 282 (M + H)⁺.

(*S*)-2-(4-Chlorophenyl)-1-(4-((5*R*,7*R*)-7-hydroxy-5-methyl-6,7-dihydro-5*H*-cyclopenta[*d*]pyrimidin-4-yl)piperazin-1-yl)-3-((2,2,2-trifluoroethyl)amino)propan-1-one Dihydrochloride Salt (37). To a solution of 12a (0.163 g, 0.531 mmol), 58a (0.170 g, 0.531 mmol), and DIEA (0.323 mL, 1.86 mmol) in 1:1 DCM–DMF (5 mL) was added HBTU (0.201 g, 0.531 mmol). The reaction mixture was stirred at rt for 1 h, after which 2 M Na₂CO₃ was added. The mixture was extracted with DCM, and the combined extracts were dried (Na₂SO₄), filtered, and concentrated. The crude was purified by silica gel column chromatography (9:1 DCM–MeOH) to give the 1:1 mixture of diastereomers, which was separated by chiral HPLC to give (*S*)-2-(4-chlorophenyl)-1-(4-((5*R*,7*R*)-7-hydroxy-5-methyl-6,7-dihydro-5*H*-cyclopenta[*d*]pyrimidin-4-yl)piperazin-1-yl)-3-((2,2,2-trifluoroethyl)amino)propan-1-one dihydrochloride (0.062 g, 20% yield): ¹H NMR (D₂O, 400 MHz) δ 8.36 (s, 1H), 7.35 (d, $J = 8.6$ Hz, 2H), 7.21 (d, $J = 8.6$ Hz, 2H), 5.25 (t, $J = 8.0$ Hz, 1H), 4.34 (dd, $J = 8.2$, 5.2 Hz, 1H), 4.16–4.04 (m, 1H), 3.90–3.40 (m, 10H), 3.32 (dd, $J = 12.8$, 5.4 Hz, 2H), 2.18 (dd, $J = 12.8$, 8.0 Hz, 1H), 2.08–1.96 (m, 1H), 0.96 (d, $J = 7.0$ Hz, 3H); LC/MS APCI (+) m/z 478.2 (M + H)⁺; HPLC (method B) 98% purity, $t_R = 2.21$ min.

General Procedure for Preparation of Compounds with Cyclic Tertiary Amines and tert-Butylamines. (*S*)-2-(4-Chlorophenyl)-3-(4-fluoropiperidin-1-yl)-1-(4-((5*R*,7*R*)-7-hydroxy-5-methyl-6,7-dihydro-5*H*-cyclopenta[*d*]pyrimidin-4-yl)piperazin-1-yl)propan-1-one (40). A solution of 4-fluoropiperidine hydrochloride (1.065 g, 7.629 mmol) in THF (10 mL) was treated with TEA (1.134 mL, 8.137 mmol) followed by the addition of methyl 2-(4-chlorophenyl)acrylate (57a; 1.000 g, 5.086 mmol). The reaction mixture was stirred at rt for 48 h. The reaction was diluted with EtOAc, washed with NaHCO₃ and brine, dried over MgSO₄, filtered, and concentrated to give methyl 2-(4-chlorophenyl)-3-(4-fluoropiperidin-1-yl)propanoate (1.521 g, 100% yield): ¹H NMR (CDCl₃, 400 MHz) δ 7.31–7.23 (m, 4H), 4.73–4.66 (m, 0.5H), 4.60–4.54 (m, 0.5H), 3.83–3.77 (dd, 1H), 3.68 (s, 3H), 3.15–3.07 (dd, 1H), 2.73–2.64 (m, 1H), 2.62–2.43 (m, 3H), 2.40–2.32 (m, 1H), 1.92–1.75 (m, 4H); LC/MS APCI (+) m/z 300.1 (M + H)⁺.

To a solution of methyl 2-(4-chlorophenyl)-3-(4-fluoropiperidin-1-yl)propanoate (0.380 g, 1.27 mmol) in THF (10 mL) was added KO(TMS) (0.199 g, 1.39 mmol). The reaction mixture was stirred at rt overnight. Additional KO(TMS) (20 mg) was added. The reaction was concentrated, and the crude product (0.232 g, 0.716 mmol) was added to a solution of 12b (0.200 g, 0.651 mmol) in DCM (4 mL). DIEA (0.363 mL, 2.08 mmol) and HBTU (0.272 g, 0.716 mmol) were added to the reaction mixture. The reaction was stirred at rt overnight and then partitioned between DCM and saturated NaHCO₃. The aqueous layer was extracted with DCM. The combined extracts were washed with brine, dried over MgSO₄, filtered, and concentrated. The residue was purified by silica gel column chromatography (12:1 DCM–MeOH) to give the 1:1 mixture of diastereomers, which was separated by chiral SFC to give (*S*)-2-(4-chlorophenyl)-3-(4-fluoropiperidin-1-yl)-1-(4-((5*R*,7*R*)-7-hydroxy-5-methyl-6,7-dihydro-5*H*-cyclopenta[*d*]pyrimidin-4-yl)piperazin-1-yl)propan-1-one (0.032 g, 10% yield): ¹H NMR (DMSO-*d*₆, 400 MHz) δ 8.44 (s, 1H), 7.39 (d, $J = 9.2$ Hz, 2H), 7.36 (d, $J = 9.2$ Hz, 2H), 5.41 (d, $J = 5.6$ Hz, 1H), 4.84 (dd, $J = 12.0$, 6.4 Hz, 1H), 4.62 (dd, $J = 49.2$, 3.2 Hz, 1H), 4.31 (dd, $J = 12.0$, 6.4 Hz, 1H), 3.74–3.72 (m, 1H), 3.64–3.60 (m, 2H), 3.54–3.28 (m, 5H), 3.02 (dd, $J = 12.4$, 8.0 Hz, 1H), 2.59–2.54 (m, 2H), 2.44 (dd, $J = 12.8$, 6.0 Hz, 1H), 2.36–2.34 (m, 2H), 1.95 (ddd, $J = 27.6$, 13.2, 6.4 Hz, 1H), 1.92 (ddd, $J = 20.4$, 13.2, 3.2 Hz, 1H), 1.79–1.76 (m, 1H), 1.73–1.70 (m, 1H), 1.13 (d, $J = 6.4$, 1H), 1.05 (d, $J = 6.8$ Hz, 3H); LC/MS APCI (+) m/z 502 (M + H)⁺; HPLC (method B) >99% purity, $t_R = 1.89$ min.

(*S*)-2-(4-Chlorophenyl)-3-((1-hydroxy-2-methylpropan-2-yl)amino)-1-(4-((5*R*,7*R*)-7-hydroxy-5-methyl-6,7-dihydro-5*H*-cyclopenta[*d*]pyrimidin-4-yl)piperazin-1-yl)propan-1-one Bis-(trifluoroacetate) Salt (39). Compound 39 was prepared from 57a and 2-amino-2-methylpropan-1-ol by the same procedure described for 40: ¹H NMR (CD₃OD, 400 MHz) δ 8.40 (s, 1H), 7.39 (d, $J = 8.0$ Hz, 2H), 7.32 (d, $J = 8.0$ Hz, 2H), 5.36 (d, $J = 6.2$ Hz, 1H), 4.84–4.79 (m, 1H), 4.39–4.36 (m, 1H), 4.30 (d, $J = 4.5$ Hz, 2H), 4.09–4.05 (m, 1H), 3.70–3.55 (m, 4H), 3.50–3.43 (m, 3H), 3.20–3.00 (m, 4H), 2.60–2.57

(m, 1H), 2.06–1.94 (m, 2H), 1.09–1.04 (m, 3H), 0.89 (d, $J = 8.0$ Hz, 6H); LC/MS APCI (+) m/z 488 (M + H)⁺; HPLC (method C) >99% purity, $t_R = 3.42$ min.

(*S*)-3-Amino-1-(4-((5*R*,7*R*)-7-hydroxy-5-methyl-6,7-dihydro-5*H*-cyclopenta[d]pyrimidin-4-yl)piperazin-1-yl)-2-(4-(trifluoromethyl)phenyl)propan-1-one Bis(trifluoroacetate) Salt (**49**). Compound **49** was prepared from 2-(4-(trifluoromethyl)acetyl chloride by the same procedure described for **34**: ¹H NMR (DMSO- d_6 , 400 MHz) δ 8.80 (s, 1H), 7.92 (d, $J = 8.0$ Hz, 2H), 7.61 (d, $J = 8.0$ Hz, 2H), 5.08 (m, 1H), 4.44–4.40 (m, 1H), 3.89–3.84 (m, 2H), 3.76–3.30 (m, 8H), 3.12 (m, 2H), 2.08 (m, 2H), 1.07 (d, $J = 8.0$ Hz, 3H); LC/MS APCI (+) m/z 450 (M + H)⁺; HPLC (method C) >99% purity, $t_R = 3.30$ min.

(*S*)-2-(4-Chloro-3-fluorophenyl)-1-(4-((5*R*,7*R*)-7-hydroxy-5-methyl-6,7-dihydro-5*H*-cyclopenta[d]pyrimidin-4-yl)piperazin-1-yl)-3-(isopropylamino)propan-1-one Dihydrochloride Salt (**50**). Compound **50** was prepared from **12b** and (*S*)-2-(4-chloro-3-fluorophenyl)-3-(isopropylamino)propanoic acid by the same procedure described for **28**: ¹H NMR (D₂O, 400 MHz) δ 8.35 (s, 1H), 7.44 (t, $J = 7.2$ Hz, 1H), 7.14 (d, $J = 9.2$ Hz, 1H), 7.04 (d, $J = 7.2$ Hz, 1H), 5.28–5.16 (m, 1H), 4.38–4.28 (m, 1H), 4.10–3.98 (m, 1H), 3.88–3.72 (m, 2H), 3.72–3.16 (m, 9H), 2.22–2.12 (m, 1H), 2.10–1.96 (m, 1H), 1.32–1.08 (m, 6H), 0.96 (d, $J = 5.6$ Hz, 3H); LC/MS APCI (+) m/z 476 (M + H)⁺; HPLC (method A) 98% purity, $t_R = 2.38$ min.

(*S*)-3-(*tert*-Butyl)-2-(3-fluoro-4-(trifluoromethyl)phenyl)-1-(4-((5*R*,7*R*)-7-hydroxy-5-methyl-6,7-dihydro-5*H*-cyclopenta[d]pyrimidin-4-yl)piperazin-1-yl)propan-1-one Bis(trifluoroacetate) Salt (**51**). Compound **51** was prepared from **57b** and *tert*-butylamine by the same procedure described for **40**: ¹H NMR (DMSO- d_6 , 400 MHz) δ 8.80 (s, 1H), 7.92 (d, $J = 8.0$ Hz, 2H), 7.61 (d, $J = 8.0$ Hz, 2H), 5.08 (m, 1H), 4.44–4.40 (m, 1H), 3.89–3.85 (m, 2H), 3.76–3.30 (m, 8H), 3.12 (m, 2H), 2.08 (m, 2H), 1.07 (d, $J = 8.0$ Hz, 3H); LC/MS APCI (+) m/z 524 (M + H)⁺; HPLC (method C) 95.3% purity, $t_R = 3.95$ min.

(*S*)-2-(3-Fluoro-4-(trifluoromethyl)phenyl)-3-((1-hydroxy-2-methylpropan-2-yl)amino)-1-(4-((5*R*,7*R*)-7-hydroxy-5-methyl-6,7-dihydro-5*H*-cyclopenta[d]pyrimidin-4-yl)piperazin-1-yl)propan-1-one Bis(trifluoroacetate) Salt (**52**). Compound **52** was prepared from **57b** and 2-amino-2-methylpropan-1-ol by the same procedure described for **40**: ¹H NMR (D₂O, 400 MHz) δ 8.58 (s, 1H), 7.86 (dd, $J = 8.0, 5.6$ Hz, 1H), 7.49 (d, $J = 8.0$ Hz, 1H), 7.36 (d, $J = 5.6$ Hz, 1H), 5.07 (m, 1H), 4.50 (m, 1H), 3.91 (m, 2H), 3.80–3.60 (m, 4H), 3.40–3.22 (m, 5H), 3.04 (m, 2H), 2.02 (m, 2H), 1.22 (m, 6H), 1.04 (d, $J = 8.0$ Hz, 6H); LC/MS APCI (+) m/z 540 (M + H)⁺; HPLC (method C) 98.3% purity, $t_R = 3.90$ min.

(*S*)-3-((Cyclopropylmethyl)amino)-2-(3-fluoro-4-(trifluoromethyl)phenyl)-1-(4-((5*R*,7*R*)-7-hydroxy-5-methyl-6,7-dihydro-5*H*-cyclopenta[d]pyrimidin-4-yl)piperazin-1-yl)propan-1-one Bis(trifluoroacetate) Salt (**53**). Compound **53** was prepared from **12b** and (*S*)-3-((cyclopropylmethyl)amino)-2-(3-fluoro-4-(trifluoromethyl)phenyl)propanoic acid by the same procedure described for **28**: ¹H NMR (DMSO- d_6 , 400 MHz) δ 8.32 (s, 1H), 7.78 (dd, $J = 8.0, 6.2$ Hz, 1H), 7.53 (d, $J = 8.0$ Hz, 1H), 7.39 (d, $J = 6.2$ Hz, 1H), 5.10–5.08 (m, 1H), 4.62–4.60 (m, 1H), 3.90–3.20 (m, 8H), 2.86 (m, 2H), 2.06–2.02 (m, 2H), 1.18–1.15 (m, 1H), 1.09 (d, $J = 8.0$ Hz, 3H), 0.59–0.54 (m, 2H), 0.33–0.29 (m, 2H); LC/MS APCI (+) m/z 522 (M + H)⁺; HPLC (method C) >99% purity, $t_R = 4.08$ min.

(*S*)-2-(4-Chloro-3-fluorophenyl)-1-(4-((5*R*,7*R*)-7-hydroxy-5-methyl-6,7-dihydro-5*H*-cyclopenta[d]pyrimidin-4-yl)piperazin-1-yl)-3-((tetrahydro-2*H*-pyran-4-yl)amino)propan-1-one Dihydrochloride Salt (**54**). Compound **54** was prepared from (*S*)-3-amino-2-(3-fluoro-4-(trifluoromethyl)phenyl)-1-(4-((5*R*,7*R*)-7-hydroxy-5-methyl-6,7-dihydro-5*H*-cyclopenta[d]pyrimidin-4-yl)piperazin-1-yl)propan-1-one and tetrahydro-2*H*-pyran-4-carbaldehyde by the same procedure described for **44**: ¹H NMR (D₂O, 400 MHz) δ 8.37 (s, 1H), 7.44 (t, $J = 7.6$ Hz, 1H), 7.15 (d, $J = 9.6$ Hz, 1H), 7.05 (d, $J = 7.6$ Hz, 1H), 5.24 (t, $J = 7.8$ Hz, 1H), 4.38–4.30 (m, 1H), 4.12–4.04 (m, 1H), 4.00–3.88 (m, 2H), 3.88–3.75 (m, 2H), 3.75–3.64 (m, 1H), 3.64–3.42 (m, 5H), 3.42–3.18 (m, 5H), 2.22–2.18 (m, 1H), 2.08–1.86 (m, 3H), 1.68–1.52 (m, 2H), 0.97 (d, $J = 6.4$ Hz, 3H); LC/MS APCI (+) m/z 518 (M + H)⁺; HPLC (method A) 98% purity, $t_R = 2.37$ min.

■ ASSOCIATED CONTENT

Supporting Information

Enzyme inhibition results (expressed as a percentage of the control) for compounds **2**, **3**, and **28** tested against a panel of 226, 225, and 230 kinases, respectively, performed at Upstate, Charlottesville, VA.¹⁵ This material is available free of charge via the Internet at <http://pubs.acs.org>.

■ AUTHOR INFORMATION

Corresponding Author

*Phone: (303) 386-1262. E-mail: jblake@arraybiopharma.com.

Notes

The authors declare no competing financial interest.

■ ABBREVIATIONS USED

AGC, cAMP-dependent protein kinase/protein kinase G/protein kinase C extended family; DAST, diethylaminosulfur trifluoride; HER2, human epidermal growth factor receptor 2; LNCaP, lymph node carcinoma of the prostate; MCF7, Michigan Cancer Foundation-7; MCT, methylcellulose with 0.2% Tween-80; mTOR, mammalian target of rapamycin; p70S6K, phosphoprotein 70 ribosomal protein S6 kinase; PBSF, *n*-perfluorobutanesulfonyl fluoride; PC3, prostate cancer cell line; PRAS40, proline-rich Akt substrate; PRKG, cyclic GMP-dependent protein kinase; PTEN, phosphatase and tensin homologue; ROCK1, ρ -associated coiled coil containing protein kinase 1; RPS6, ribosomal protein S6; shRNA, short hairpin RNA; TsDPEN, tosyl-1,2-diphenylethylene

■ REFERENCES

- (a) Cheng, J. Q.; Lindsley, C. W.; Cheng, G. Z.; Yang, H.; Nicosia, S. V. The Akt/PKB pathway: molecular target for cancer drug discovery. *Oncogene* **2005**, *24*, 7482–7492. (b) Manning, B. D.; Cantley, L. C. AKT/PKB signaling: navigating downstream. *Cell* **2007**, *129*, 1261–1274.
- (a) Altomare, D. A.; Testa, J. R. Perturbations of the AKT signaling pathway in human cancer. *Oncogene* **2005**, *24*, 7455–7464. (b) Vivanco, I.; Sawyers, C. L. The phosphatidylinositol 3-kinase AKT pathway in human cancer. *Nat. Rev. Cancer* **2002**, *2*, 489–501. (c) Lian, Z.; Di Cristofano, A. Class reunion: PTEN joins the nuclear crew. *Oncogene* **2005**, *24*, 7394–7400.
- (3) Degtyarev, M.; De Mazière, A.; Orr, C.; Lin, J.; Lee, B. B.; Tien, J. Y.; Prior, W. W.; van Dijk, S.; Wu, H.; Gray, D. C.; Davis, D. P.; Stern, H. M.; Murray, L. J.; Hoeflich, K. P.; Klumperman, J.; Friedman, L. S.; Lin, K. Akt inhibition promotes autophagy and sensitizes PTEN-null tumors to lysosomotropic agents. *J. Cell Biol.* **2008**, *183*, 101–116.
- (a) Chen, Y. L.; Law, P. -Y.; Loh, H. H. Inhibition of PI3K/Akt signaling: an emerging paradigm for targeted cancer therapy. *Curr. Med. Chem. Anticancer Agents* **2005**, *5*, 575–589. (b) Lu, Y.; Wang, H.; Mills, G. B. Targeting PI3K-AKT pathway for cancer therapy. *Rev. Clin. Exp. Hematol.* **2003**, *7*, 205–228. (c) Mitsiades, C. S.; Mitsiades, N.; Koutsilieris, M.; Nicholson, K. M.; Anderson, N. G.; Neri, L. M.; Borgatti, P.; Capitani, S.; Martelli, M.; Brazil, D. P.; Hemmings, B. A. The Akt pathway: molecular targets for anti-cancer drug development. *Curr. Cancer Drug Targets* **2004**, *4*, 235–256.
- (5) Pal, S. K.; Reckamp, K.; Yu, H.; Figlin, R. A. Akt inhibitors in clinical development for the treatment of cancer. *Expert Opin. Invest. Drugs* **2010**, *19*, 1355–1366.
- (6) Blake, J. F.; Kallan, N. C.; Xiao, D.; Xu, R.; Bencsik, J. R.; Skelton, N. J.; Spencer, K. L.; Mitchell, I. S.; Woessner, R. D.; Gloor, S. L.; Risom, T.; Gross, S. D.; Martinson, M.; Morales, T. H.; Vigers, G. P. A.; Brandhuber, B. J. Discovery of pyrrolopyrimidine inhibitors of Akt. *Bioorg. Med. Chem. Lett.* **2010**, *20*, 5607–5612.
- (7) Bencsik, J. R.; Xiao, D.; Blake, J. F.; Kallan, N. C.; Mitchell, I. S.; Spencer, K. L.; Xu, R.; Gloor, S. L.; Martinson, M.; Risom, T.; Woessner,

R. D.; Dizon, F.; Wu, W.-I.; Vigers, G. P. A.; Brandhuber, B. J.; Skelton, N. J.; Prior, W. W.; Murray, L. J. Discovery of dihydrothieno- and dihydrofuroypyrimidines as potent pan Akt inhibitors. *Bioorg. Med. Chem. Lett.* **2010**, *20*, 7037–7041.

(8) Taber, D. F.; Petty, E. H. General route to highly functionalized cyclopentane derivatives by intermolecular C–H insertion. *J. Org. Chem.* **1982**, *47*, 4808–4809.

(9) Nugent, W. A.; Hobbs, F. W., Jr. Improved route to 3-vinyl substituted cyclopentanones. Synthesis of (\pm)-mitsugashiwalactone. *J. Org. Chem.* **1986**, *51*, 3376–3378.

(10) Yin, J.; Zarkowsky, D. S.; Thomas, D. W.; Zhao, M. M.; Huffman, M. A. Direct and convenient conversion of alcohols to fluorides. *Org. Lett.* **2004**, *6*, 1465–1468.

(11) Fujii, A.; Hashiguchi, S.; Uematsu, N.; Ikariya, T.; Noyori, R. Ruthenium (II)-catalyzed asymmetric transfer hydrogenation of ketones using a formic acid–triethylamine mixture. *J. Am. Chem. Soc.* **1996**, *118*, 2521–2522.

(12) Middleton, W. J. New fluorinating reagents. Dialkylaminosulfur fluorides. *J. Org. Chem.* **1975**, *40*, 574–578.

(13) (a) Matsumura, Y.; Kanda, Y.; Shirai, K.; Onomura, O.; Maki, T. A convenient method for synthesis of enantiomerically enriched methylphenidate from *N*-methoxycarbonylpiperidine. *Org. Lett.* **1999**, *1*, 175–178. (b) Matsumura, Y.; Kanda, Y.; Shirai, K.; Onomura, O.; Maki, T. A convenient method for synthesis of optically active methylphenidate from *N*-methoxycarbonylpiperidine by utilizing electrochemical oxidation and Evans aldol-type reaction. *Tetrahedron* **2000**, *56*, 7411–7422. (c) Pilli, R. A.; Böckelmann, M. A.; de Fatima Alves, C. The stereochemistry of the addition of chlorotitanium enolates of *N*-acyl oxazolidin-2-ones to 5- and 6-membered *N*-acyliminium ions. *J. Braz. Chem. Soc.* **2001**, *12*, 634–651.

(14) Kallan, N. C.; Spencer, K. L.; Blake, J. F.; Xu, R.; Heizer, J.; Bencsik, J. R.; Mitchell, I. S.; Gloor, S. L.; Martinson, M.; Risom, T.; Gross, S. D.; Morales, T. H.; Vigers, G. P. A.; Brandhuber, B. J.; Skelton, N. J. Discovery and SAR of spirochromane Akt inhibitors. *Bioorg. Med. Chem. Lett.* **2011**, *21*, 2410–2414.

(15) The inhibition against a panel of kinases was determined at Upstate, Charlottesville, VA.

(16) The crystallographic data described have been deposited with the RCSB Protein Data Bank (PDB code for **28**, 4EKL).

(17) Milletti, F.; Storchi, L.; Goracci, L.; Bendels, S.; Wagner, B.; Kansy, M.; Cruciani, G. Extending pK_a prediction accuracy: high-throughput pK_a measurements to understand pK_a modulation of new chemical series. *Eur. J. Med. Chem.* **2010**, *45*, 4270–4279.

(18) Zeng, Q.; Bourbeau, M. P.; Wohlhieter, G. E.; Yao, G.; Monenschein, H.; Rider, J. T.; Lee, M. R.; Zhang, S.; Lofgren, J.; Freeman, D.; Li, C.; Tominey, E.; Huang, X.; Hoffman, D.; Yamane, H.; Tasker, A. S.; Dominguez, C.; Viswanadhan, V. N.; Hungate, R.; Zhang, X. 2-Aminothiadiazole inhibitors of AKT1 as potential cancer therapeutics. *Bioorg. Med. Chem. Lett.* **2010**, *20*, 1652–1656.

(19) Han, E. K.-H.; Levenson, J. D.; McGonigall, T.; Shah, O. J.; Woods, K. W.; Hunter, T.; Giranda, V. L.; Luo, Y. Akt inhibitor A-443654 induces rapid Akt Ser-473 phosphorylation independent of mTORC1 inhibition. *Oncogene* **2007**, *26*, 5655–5661.

(20) Rhodes, N.; Heerding, D. A.; Duckett, D. R.; Eberwein, D. J.; Knick, V. B.; Lansing, T. J.; McConnell, R. T.; Gilmer, T. M.; Zhang, S. Y.; Robell, K.; Kahana, J. A.; Geske, R. S.; Kleymenova, E. V.; Choudhry, A. E.; Lai, Z.; Leber, J. D.; Minthorn, E. A.; Strum, S. L.; Wood, E. R.; Huang, P. S.; Copeland, R. A.; Kumar, R. Characterization of an Akt kinase inhibitor with potent pharmacodynamic and antitumor activity. *Cancer Res.* **2008**, *68*, 2366–2374.

(21) Grimshaw, K. M.; Hunter, L. J.; Yap, T. A.; Heaton, S. P.; Walton, M. I.; Woodhead, S. J.; Fazal, L.; Reule, M.; Davies, T. G.; Seavers, L. C.; Lock, V.; Lyons, J. F.; Thompson, N. T.; Workman, P.; Garrett, M. D. AT7867 is a potent and oral inhibitor of AKT and p70 S6 kinase that induces pharmacodynamic changes and inhibits human tumor xenograft growth. *Mol. Cancer Ther.* **2010**, *9*, 1100–1110.

(22) Lin, K.; Lin, J.; Wu, W.-I.; Ballard, J.; Lee, B. B.; Gloor, S. L.; Vigers, G. P. A.; Morales, T. H.; Friedman, L. S.; Skelton, N. J.;

Brandhuber, B. J. An ATP-site on-off switch that restricts phosphatase accessibility of Akt. *Sci. Signaling* **2012**, *5*, ra37.

(23) Zaki, M. H.; Nemeth, J. A. CNTO 328, a monoclonal antibody to IL-6, inhibits human tumor-induced cachexia in nude mice. *Int. J. Cancer* **2004**, *111*, 592–595.